



EUROPEAN      SOUTHERN      OBSERVATORY

Organisation Européenne pour des Recherches Astronomiques dans l'Hemisphère Austral  
Europäische Organisation für astronomische Forschung in der südlichen Hemisphäre

# VERY LARGE TELESCOPE

## HARPS Detector final design

DOC. No: VLT-TRE-ESO-XXXX-XXXXXX

ISSUE No: 1.0

DATE: 07-Mar-01

Prepared: C.CAVADORE 07-Mar-01  
.....  
..... Date Signature

Approved: X 07-Mar-01  
.....  
..... Date Signature

Released: X 07-Mar-01  
.....  
..... Date Signature

## **1. The CCD**

The usable optical field is around 60 by 60 mm in the range of 380nm to 690nm, requiring large thinned device, either a 4x4K (15  $\mu\text{m}$  pixels) or a mosaic of two 2x4K CCDs. In that scope, and according to the devices available at ESO/ODT, the best combination for this application is more likely two 2x4K EEV44-82 CCDs.

### **1.1. EEV CCD performance overview**

#### **1.1.1. Generality**

The company EEV supplied ESO with many custom designed CCD called EEV44-82. This CCD has been used in many systems at ESO, such as GIRAFFE, FEROS, WFI, VLTC2, UVES, VIMOS ... This device has 2 readout ports. The CCD can be operated either in dual readout mode using two ports, or single port readout. Binning along the X and Y direction is possible provided that the scene is not oversaturated. A fast wiping of the device can be achieved by using a dump gate close to the serial register.

This table summarizes main CCD geometrical dimension.

<b>EEV 44-82</b>	Full Frame / Frame transfer capable	
Type : Backside, Single layer AR	Pixel size 15x15 $\mu\text{m}$ 100% photosensitive	
Number of photosensitive pixels	2048 x 4102 [HxV]	Number of outputs : 2
Size of the photosensitive area	30.72 x 61.53 mm	
Horizontal pre-scan pixels	50	

This device is 3 sides buttable. For each device, the theoretical non sensitivity side area is 100 microns and the Left-Right gaps are 450 microns each (see mosaicing section for more details).

#### **1.1.2. Noise**

The following table shows noise performances achieved with FIERA at different readout speeds and conversion factors ( $e^-/\text{ADU}$ ).

Readout Noise / Conversion factor				
<i>Speed (kps)</i>	<i>Conversion factor (<math>e^-/\text{ADU}</math>)</i>	<i>Time to readout the full 4x4K array using one port per CCD (sec)</i>	<i>Time to readout the full 4x4K array using two port per CCD (sec)</i>	<i>Noise (<math>e^- \text{ rms}</math>)</i>
50	0.54	170	85	1.9 to 2.7 *
225	0.54	38	19	3.1 to 3.8 *
625	1.64	14	7	4.5 to 5.2 *
1000	2.1	9	4.5	10

\* = These noise figures may vary slightly according to the device used.

#### **1.1.3. Quantum efficiency**

EEV has optimized the QE to get good QE in the B and U bands. Nevertheless, depending on the device, the QE in this range may vary slightly. The explanation is the following: the Quantum Efficiency of these devices is strongly related to of the thickness backside Anti-Reflection coating and this thickness may vary according to the device (Hafnium Oxide 50nm). ESO measured 12 devices and used to achieve a statistic QE plot (*figure 1.1.3*). This is a criterion also to sort science grade devices : the best QE in the blue (except for application requiring a higher red sensitivity). In the case of HARPS, no requirements are set below 360/370 nm. The best QE to achieve is between 370-900 nm.

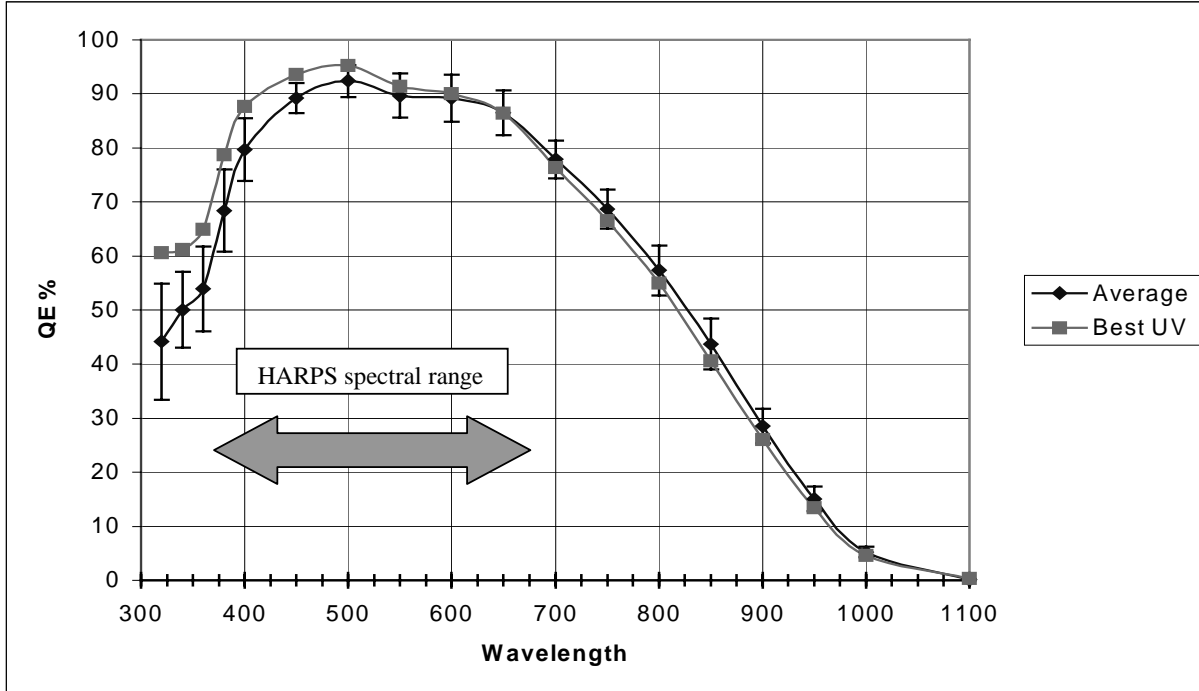


*figure 1.1.3: Average QE of 12 devices, error bars shows the QE standard deviation from these 12 devices. Also the best blue sensitive device is plotted.*

#### 1.1.4. Fringing

Fringing is an issue for spectroscopic purposes. ESO Optical Detector Team (ODT) has measured this effect with 8 devices. The resulting parameter is called Photo-Response Non-Uniformity (PRNU) across the chip (*figure 1.1.4a*). The near IR PRNU depends upon the fringing effect. This effect is related to the thinning of the CCD, and also to the aperture of the incoming beam, the more this beam is open, the less the fringing is visible. In the blue part of the spectrum the PRNU degrades also due to the backside p+ implementation laser annealing. The images (*figure 1.1.4b*) show qualitatively these effects. Figure C is a statistical analysis over 8 CCDs.

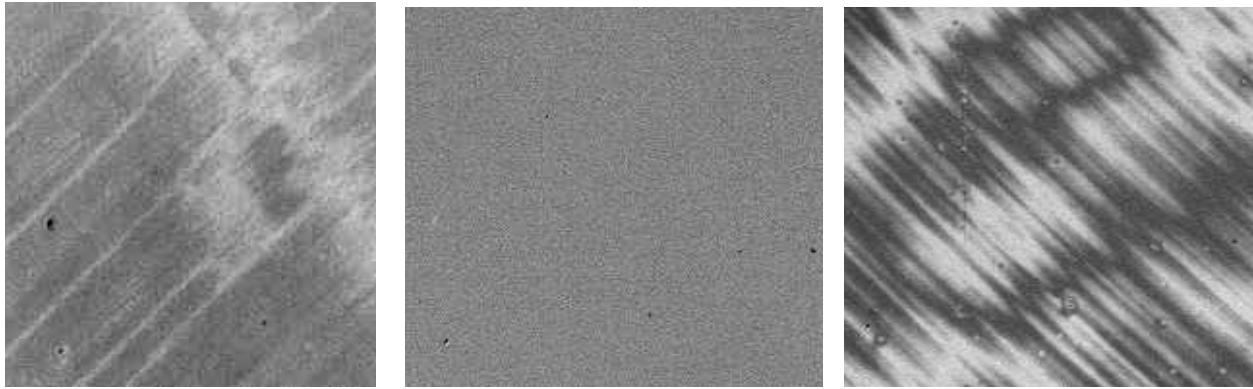


*figure 1.1.4a : Flat fields from the same area at different wavelengths, 5nm bandwidth, parallel incoming beam, left 320nm, middle 650nm, right 950nm, F/2 beam.  
300x300 pixels POSITIVE IMAGES*

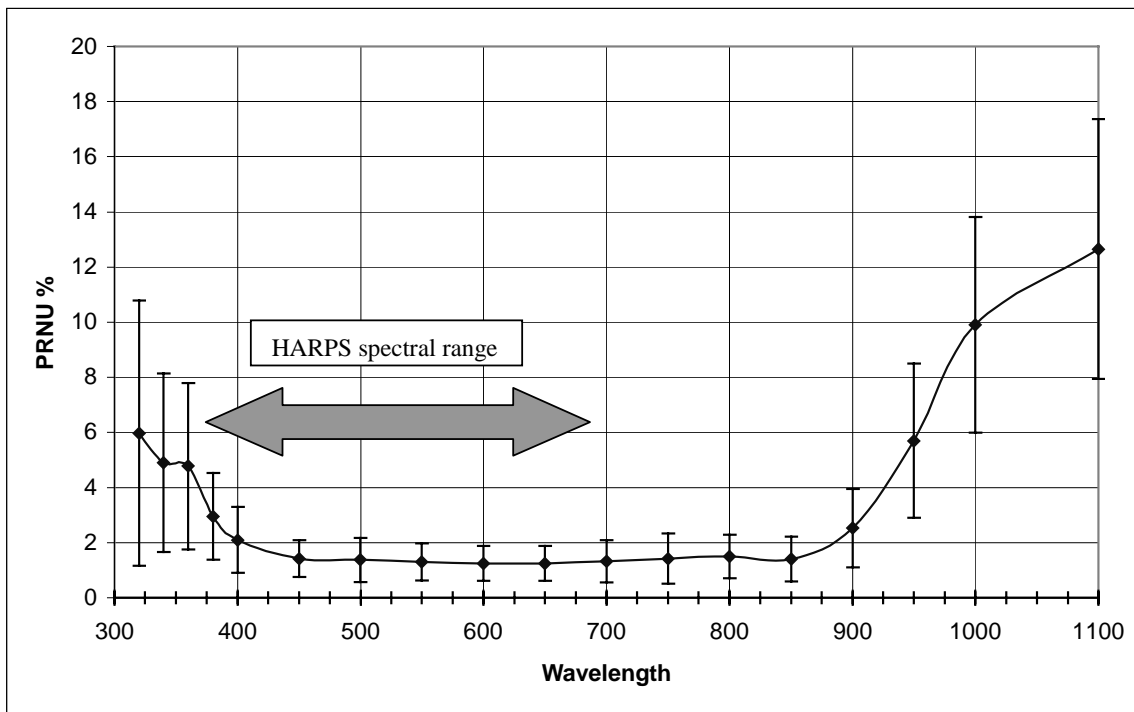


*figure 1.1.4b : Average PRNU form 8 devices, error bars shows the PRNU standard deviation from these 8 devices, F/2 beam and 5nm bandwidth.*

### **1.1.5. Cosmetic defects**

The different kind of defects, which degrade the cosmetic quality of the device, can be split in three parts :

- Defects visible in the bias images (mainly hot pixels, making bad columns)
- Defect visible with a low light level flat field (traps, making bad columns, *figure 1.1.5c*)
- Defects visible in the median stack of 5 1h exposed dark frame (mainly oversaturated hot pixels making trails, bad columns or clusters of bad pixels, *figure 1.1.5a,b*)

A defect is a pixel value above or below 5 sigmas from the mean of the neighborhood pixels.

These defects are based upon the grading of the device, typically a good science grade is one with less than 5 defective columns, the best ones have no traps, and after 1 hour exposure only 1 to 3 bad columns. The amount of defects visible on long dark exposure is strongly related to the CCD temperature. An operating CCD temperature of -120C is used to minimize these effects.

Also the CCD device is made of 1024x512 blocks, and the area boundaries show sometime a 1% QE variation over 1 row/column due to photolithography stepper mismatches. These small defects flat-field out to the photon's noise level. Trap defects are a determining factor for assigning devices to certain applications. These kind of defects cannot be suppressed because they are created during chip fabrication, and are not temperature dependent.

Finally, the amount of the "defects" induced by cosmic rays should not be more than the one provided by natural radioactivity. The CCD package and the head of the detector do not add additional hits. This value is typically between 1 and 1.5 event/min/cm<sup>2</sup> which means in a typical ½ hour exposure there will 550-600 events in the whole chip.

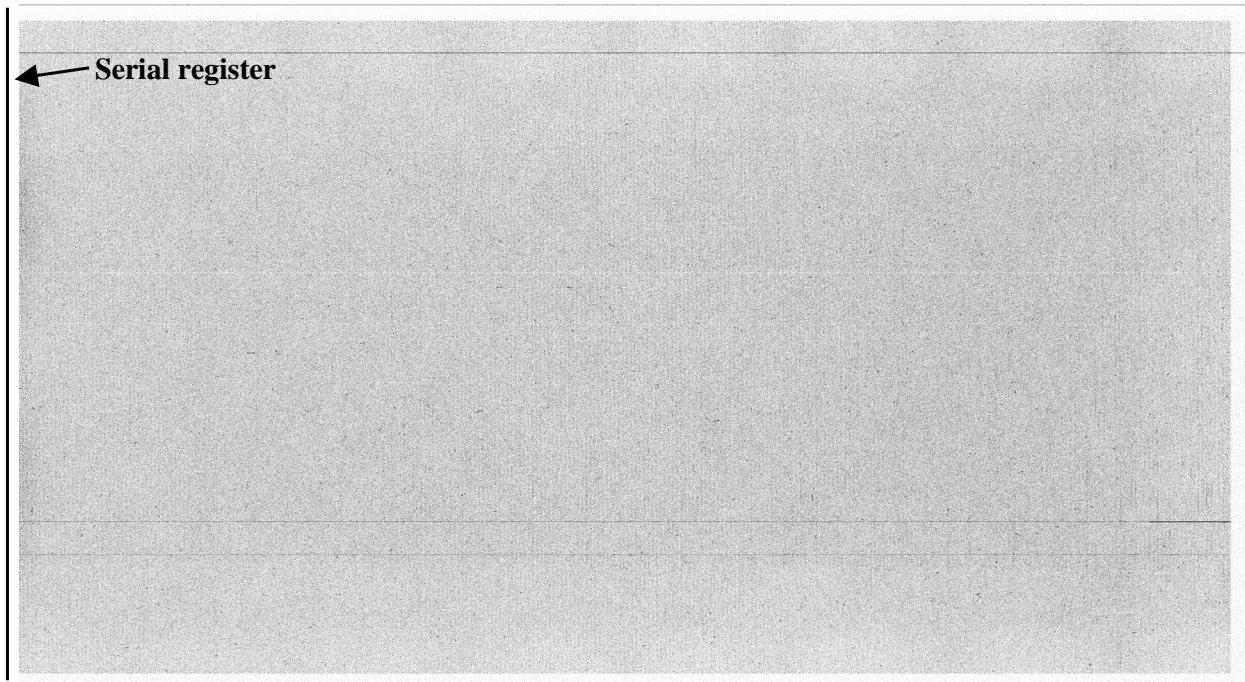


*Figure 1.1.5a, Median stacked of 1 hour exposure dark full frame of a science grade device (CCD ranked for spectroscopy) at -120C, only 3 hot columns are visible (overview of the entire device)*

**NEGATIVE IMAGE**

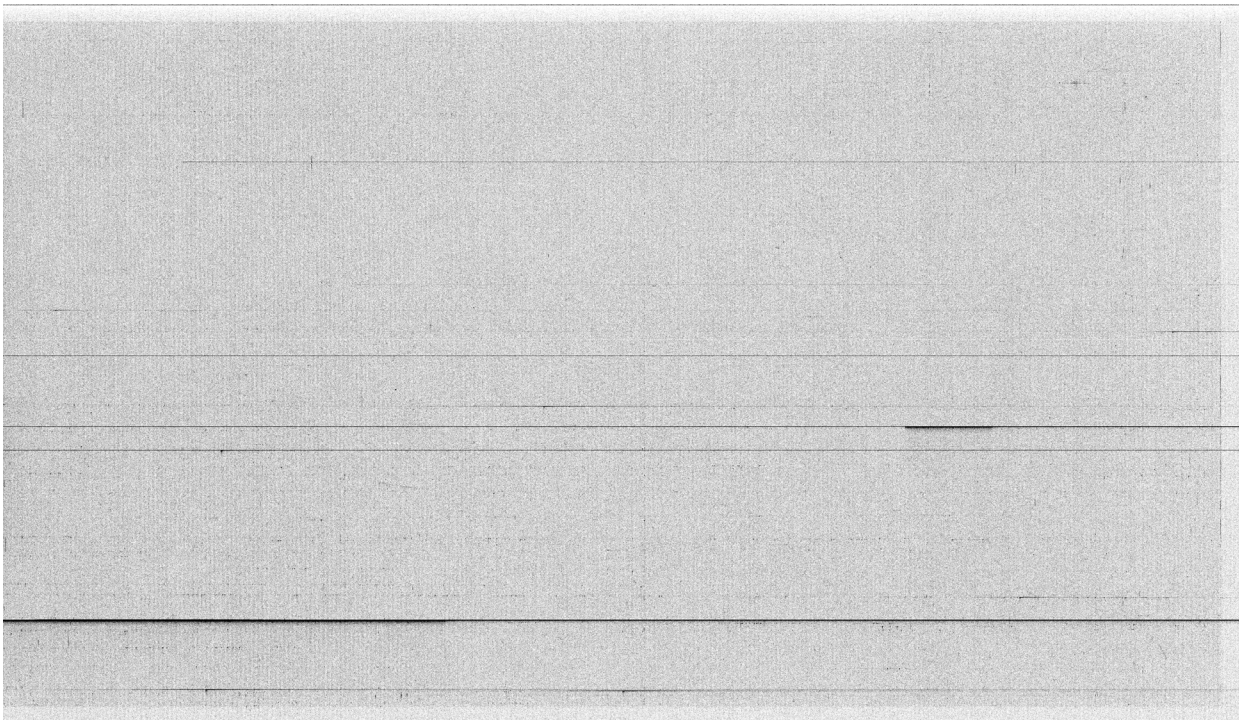


Figure 1.1.5b, Median stacked of 1 hour exposure dark frame of a medium grade device (CCD ranked for direct imaging) at -120C, 8 hot columns are visible (overview of the entire device)  
**NEGATIVE IMAGE.**

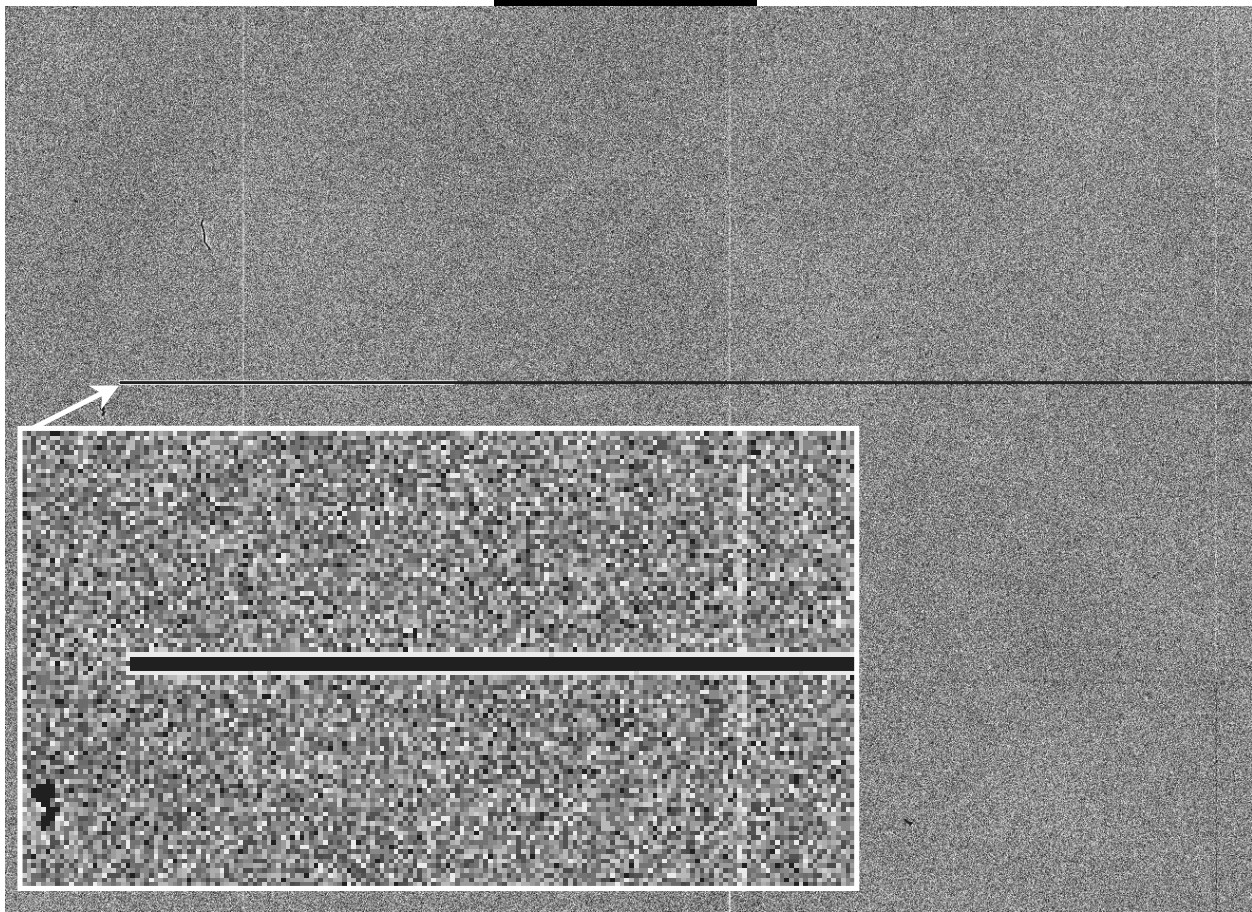


Figure 1.1.5c, Low light level frame (2000e-): a 5 column wide trap is visible here (overview of 1300x900 pixels). This device is rejected for spectroscopic applications.  
**POSITIVE IMAGE**

### **1.1.6. Charge transfer efficiency**

ESO measurements shows horizontal CTE of 0.9999995 (six 9s, 5) and vertical CTE of 0.9999988 (almost six 9s). It means in the worst case : A pixel having 1000 electrons located on the opposite side to the readout port (X=2048, Y=4100) will lose 6 electrons, once the charge packet will reach the readout node (photon shot noise is about 31e<sup>-</sup> at that level).

### **1.1.7. Dark current**

EEV44-82 devices do not have a MPP implant. The dark current is temperature dependent as shown in figure 1.1.7 . The CCD must be cooled at a temperature less than -95C for science purposes to achieve a dark current less and equal to 10 e-/pixel/hour. The ESO theoretical curve is a best fit according to the law :

$$D_k = K_1 * T^{3.2} * e^{-K_2/T}$$

K<sub>1</sub> and K<sub>2</sub> are constant which fits as best as possible the measurements, T temperature and D<sub>k</sub> dark current in e-/hour/pixel.

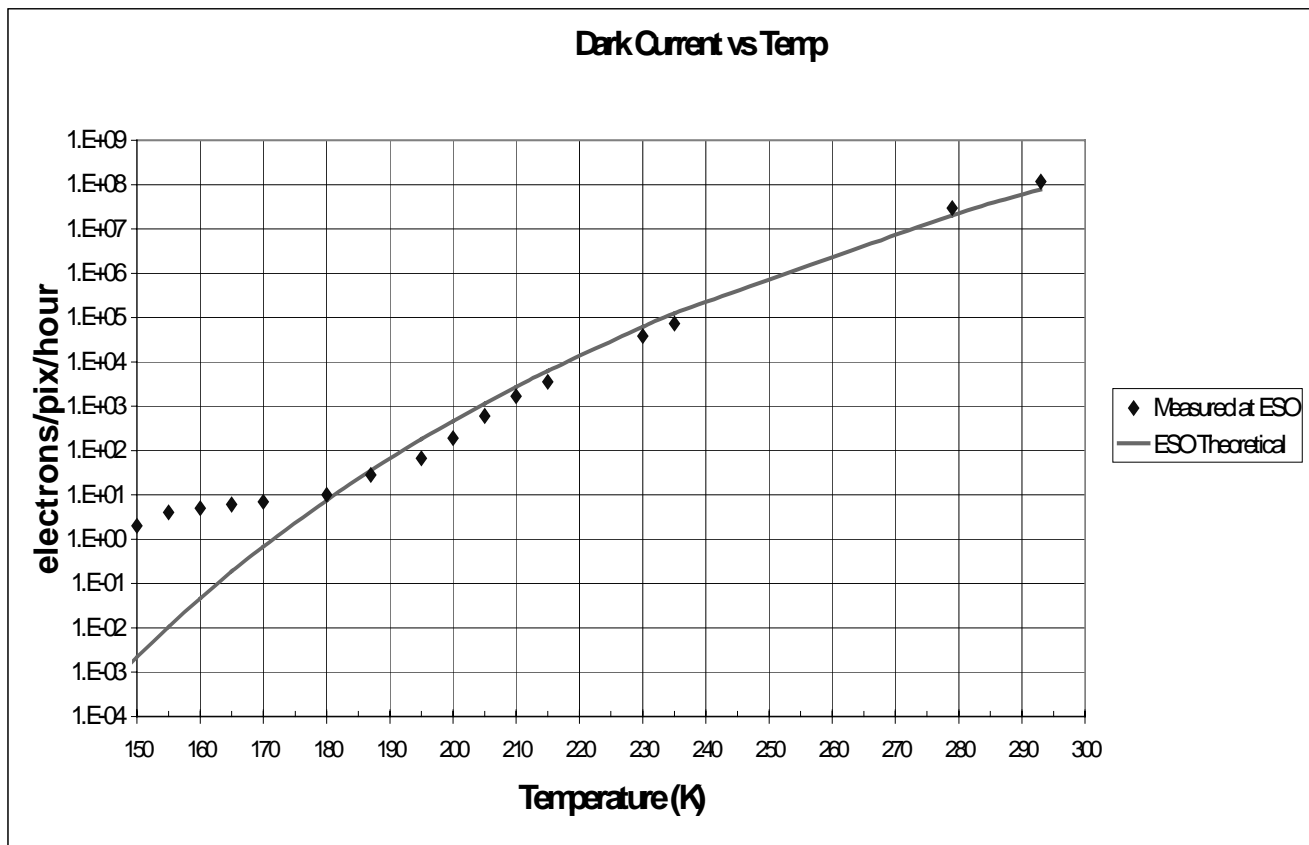


Figure 1.1.7: Dark current versus temperature

At low temperature <180K, the measurements does not match to the theoretical curve due to remanence (see section about “remanence effects”).

Temperature measured on CCD package (Celsius/K)	Dark current (e-/pix/hour)
- 102 / 171	Less than 10
- 120 / 153	1 - 2

### **1.1.8. Amplifier glowing on long exposure**

To avoid amplifier glowing, voltages less than 25 volts must be set to the VOD node of the chip.

### **1.1.9. Remanence/residual image effects**

Remanence effects may occur, if a flat field frame (Mean > 10000e-) is taken prior to the dark frame. The resulting effect resembles an increase of dark current, especially at temperatures lower than 180K. ODT is currently investigating to cure this problem. Figure H, shows a set of 24 dark frames exposed each one-hour (CCD temperature : 160K). This set was taken after the **whole** CCD was exposed to the ambient light. It requires four 1 hour darks frames to eliminate of the remanence and to reach the actual dark current value (about 5e-/pix/hour).

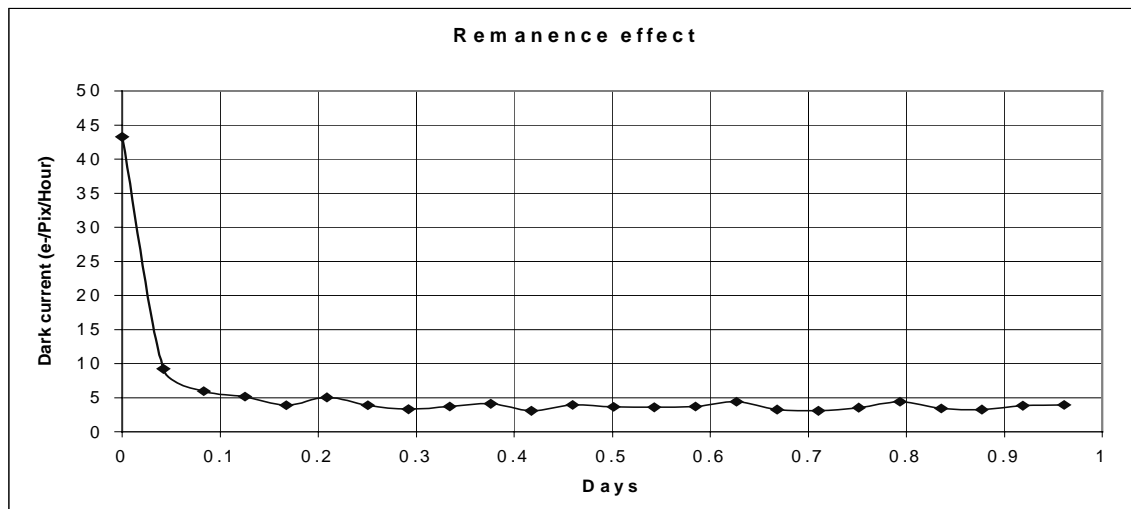


*figure 1.1.9: Remanence effect*

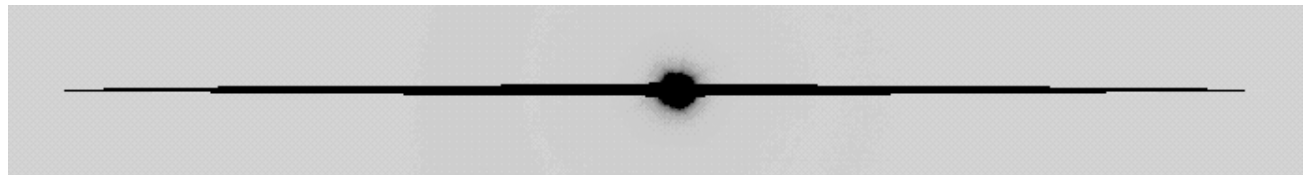


*figure 1.1.9a : oversaturated spot,  
negative image*

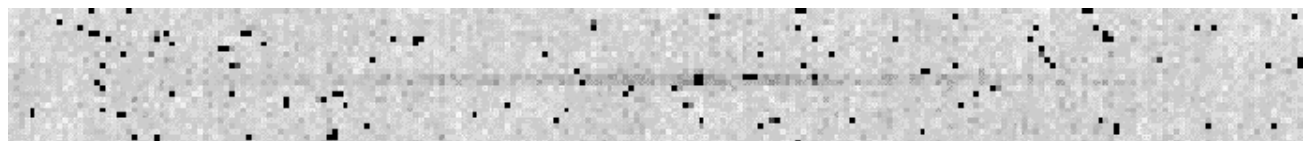


*figure 1.1.9b : one hour dark exposure, just after 1.1.9a figure, binned 10x10, plus cosmic hits,  
negative image*

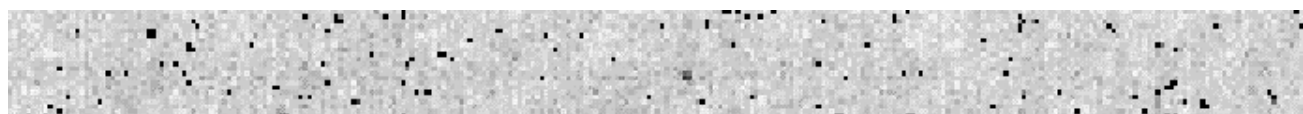


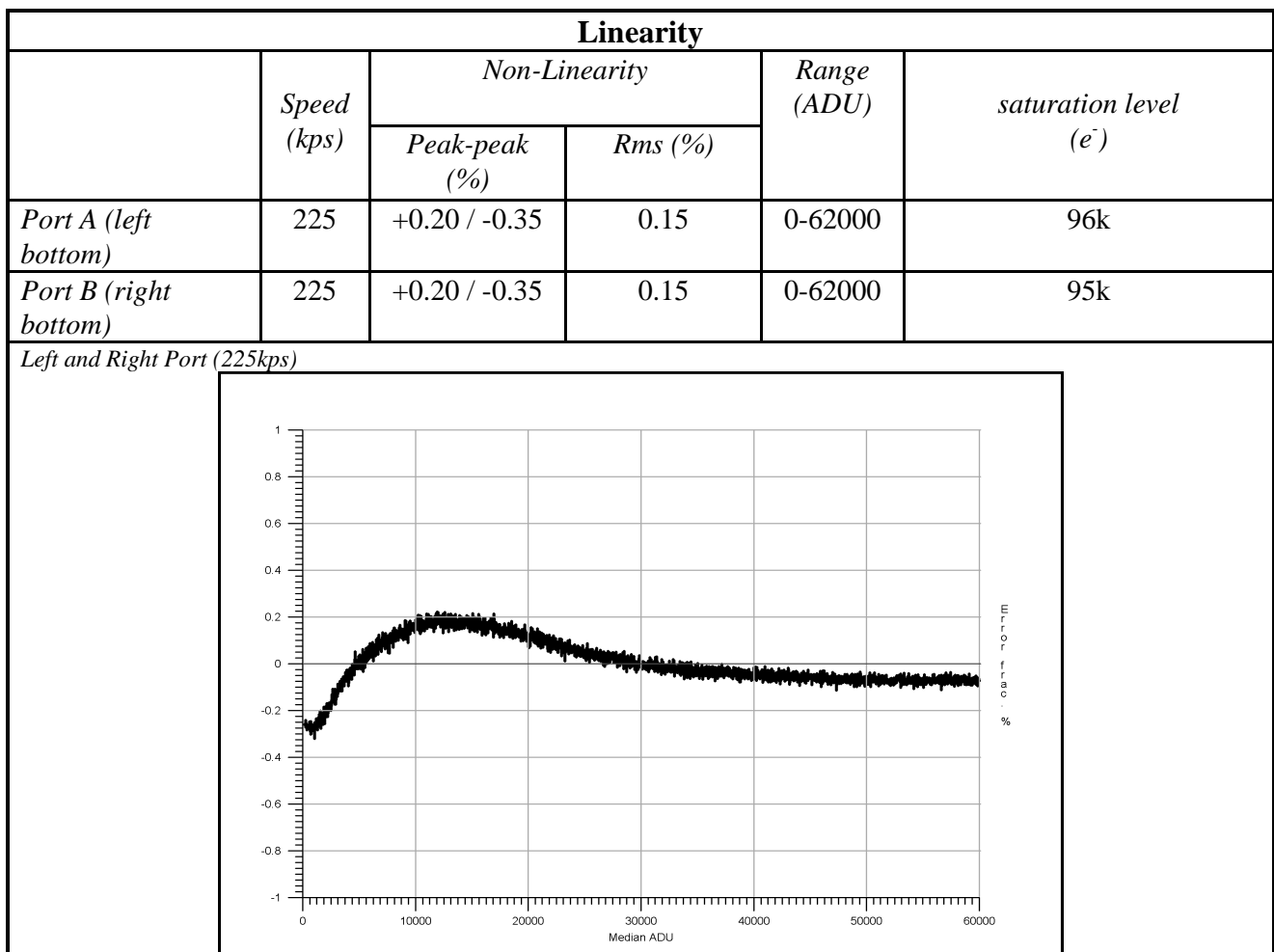
*figure 1.1.9c : one hour dark exposure, just after 1.1.9b figure, binned 10x10, only the central spot is  
visible, negative image*

Bright Star/bright spots remanent might be also visible when doing long exposure afterward. Figure *Ha* shows an oversaturated star, with intense vertical blooming. Figure *1.1.9b* shows one hour dark exposure taken just after at -120C. The blooming and central spot ghost are still visible. If additional images are taken, it disappears after 4 hours. From that study, It means that remanence has a global and local effects.

	T+1h	T+2h	T+3h
Central Bulb remanent (e-)	8	6	2
Blooming remanent (e-)	2	1	0

### 1.1.10. Linearity

By optimizing the voltages applied to the CCD readout amplifier, a good linearity can be achieved in the range of 0-100Ke<sup>-</sup> without degrading noise performance. The table below summarizes a typical linearity performance from an EEV device at 225Kps.



Best performance is achieved with p-p linearity of  $\pm 0.35\%$ . Special voltage optimisation is performed to get  $\pm 0.5\%$  at least across the full intrinsic CCD range. The intrinsic dynamic range of the CCD, at 130Ke<sup>-</sup> can be achieved; knowing that the conversion factor is around 2.0-2.2 e-/ADU with a degraded

noise level. Best noise performance is reached with 0.7e-/ADU leading to a dynamic of 40Ke- limited by the ANALOG to DIGITAL converter (65535 counts).

### **1.1.11. Flatness**

ODT has developed a special measurement device to acquire full chip surface profile. A typical value is typically  $\pm 6$  microns at 150K, a maximum value is  $\pm 10$  microns p-p.

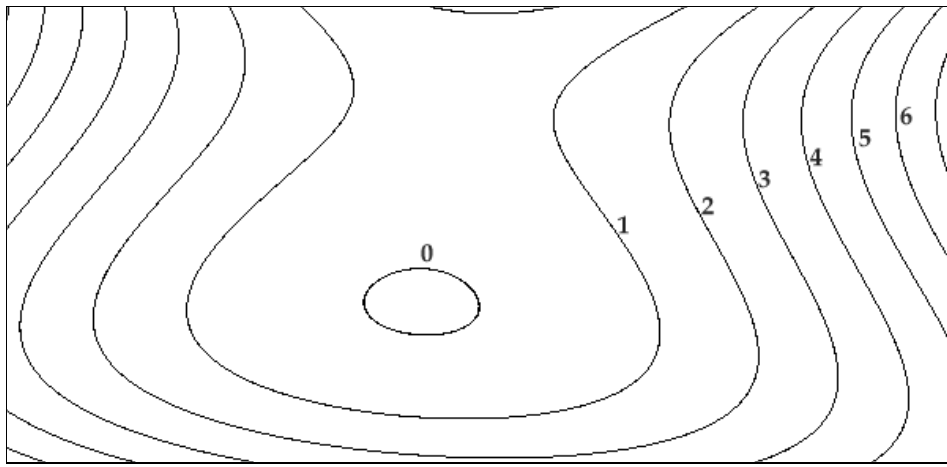


*figure 1.1.11a : Typical iso-elevation 2D plot of the CCD surface (units are microns).*

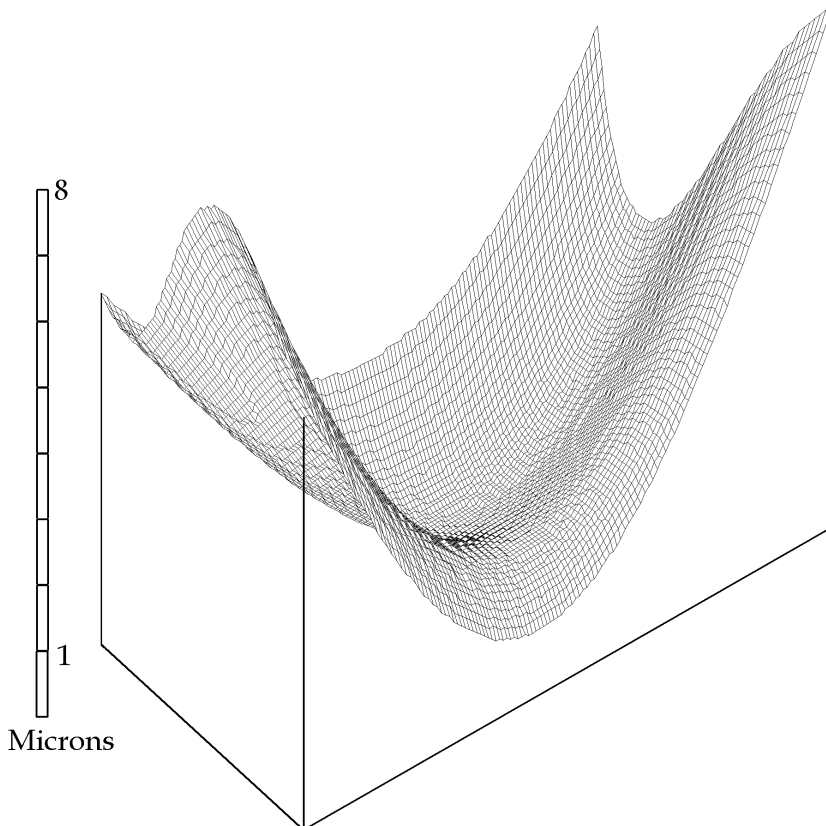


*figure 1.1.11b : Typical 3D plot of the same CCD surface as above.*

### **1.1.12. Modulation Transfer Fonction**

According to ODT's latest measurements, the CCD shows no serious degradation from the Nyquist curve. The very sharp hits resulting from the cosmic ray impacts show that 95% of the energy released is within one pixel. Up to now, no MTF absolute quantitative measurements have been undertaken.

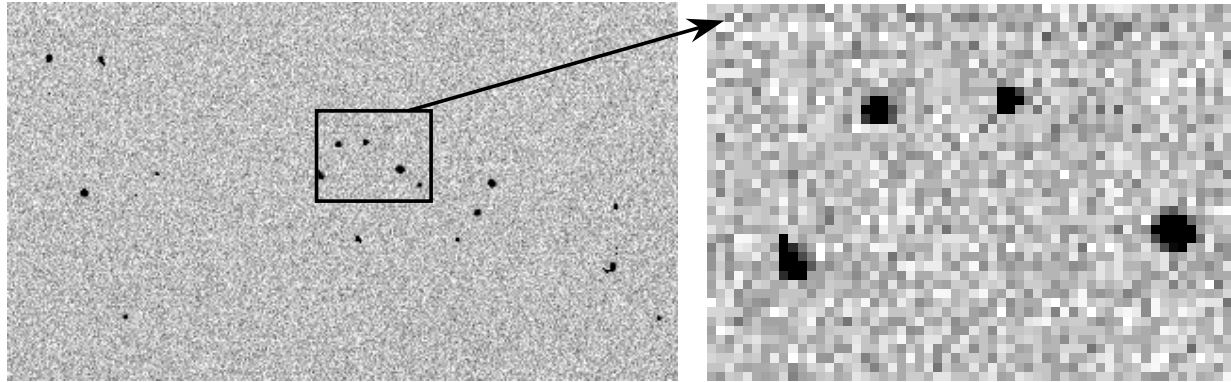


*figure 1.1.12 : Cosmic rays hits (1 hour exposure), enlargement showing 4 cosmic rays hits  
NEGATIVE IMAGE.*

PSF has been measured by the use of a F/2.5 diffraction limited optical setup, which allows producing a spot of  $5\mu\text{m}$  at different wavelengths. The sharpest spot is achieved by moving the optical setup into XYZ micrometric stage. The intensity of the brightest pixel is then measured and divided by the sum of all the pixels of the spot : this measurement gives a kind of encircled energy within a single pixel.

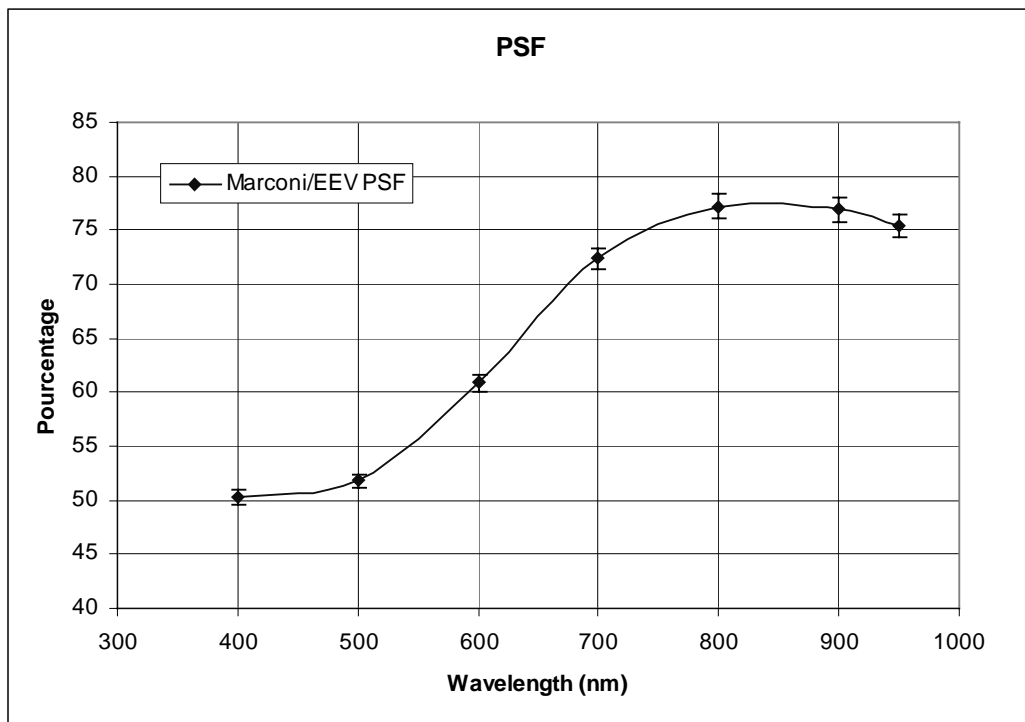


*figure 1.1.12a : PSF vs wavelength*

As expected, at 400nm, a single pixel contains 55% of all the spot energy, whereas at 800nm, it contains 75%. This is consistent with the fact that blue light is turned into photo-electrons at CCD's surface (few

angstroms) and photo-electrons have to travel a large field free region before being captured by the pixel potential well.

### **1.1.13. Binning eclipse effect on saturated stars**

When using binning more than 1x1, a saturated star appears with a strange black hole in the middle. The CCD JFET output amplifier is, in this particular state, completely out of range and behaves strangely. As there is, anyway, no useful information in the center of a saturated star (no photometry/astrometry feasible), this effect is more a cosmetic issue (which could be eliminated by software) than scientific.

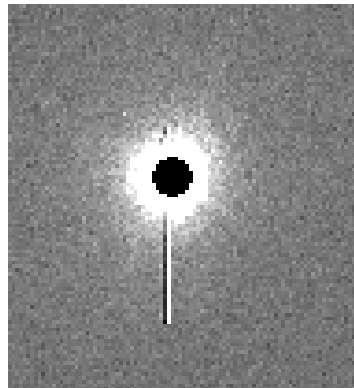


*figure 1.1.13 : Eclipse effect on a saturated star with binning 2x2  
POSITIVE IMAGE.*

### **1.1.14. Blooming effect**

This CCD does not have antiblooming implant. This causes vertical trails over bright and saturated stars. The table below gives a crude indication of the order of magnitude for point sources. L1 denotes the number of pixels concerned toward the serial register, L2 the one in the opposite direction. Measurements made with binning 1x1.

Direction	Overexposure factor							
	2	4	5.8	10	25	50	100	1000
L1(pixels)	0	0	1	2	8	19	39	344
L2(pixels)	0	0	1	3	5	8	13	136

### **1.1.15. Cross talk effect**

This CCD allowing two port readout in the same time could exhibit cross talk between the two channels. It could be visible when a bright star is present over the CCD. This effect has been measured at ESO. If an over saturated bright spot is projected over one side of the CCD, ghost having an additional fix level of 100 e- is visible on the other side, with the same shape of the original bright spot. The source of this feature is not FIERA but the CCD itself. Since this mode is used for HARPS, one has to be aware that this effect may lead to ghost lines coming from saturated one.

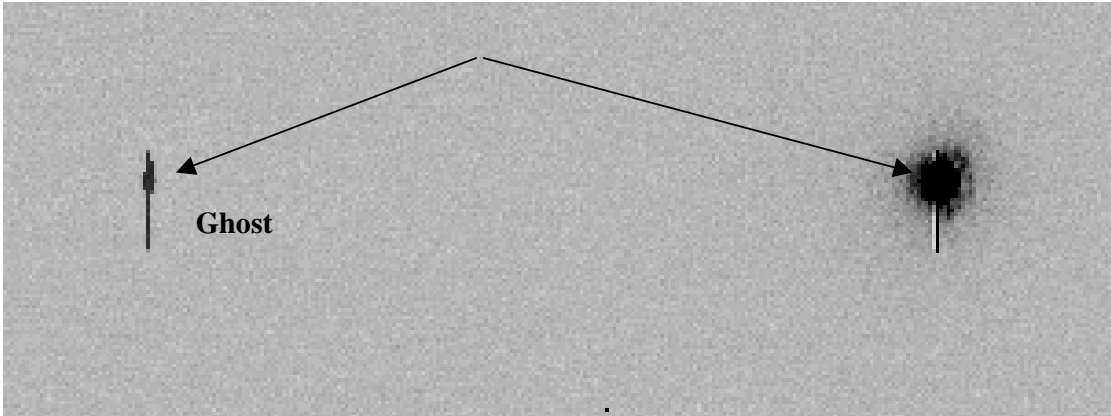


*figure 1.1.15 : Cross talk with a 50 times oversaturated star and 2 port readout, leading to 2ADU per 65535 of cross talk.*

**NEGATIVE IMAGE**

### **1.1.16. 512x1K CCD block stitching**

To be able to achieve large CCD, EEV employs a method, which consists of butting a master lithographic block of 1024x512 pixels. This builds up a CCD made of 16 of these master blocks (Figure 1.1.16a). At the boundaries of these blocks, the pixel size is not exactly 15 $\mu$ m. This pixel size variation can be measured with a flat field : large pixels make brighter lines and smaller makes darker lines (1.1.16b).

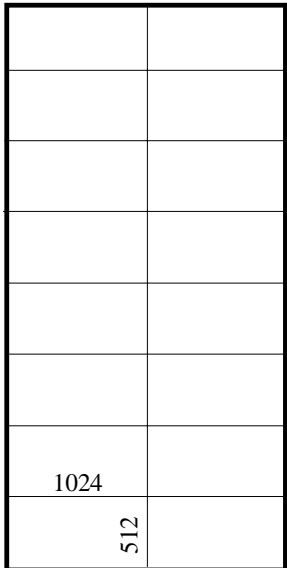


*Fig 1.1.16a CCD stitching pattern*

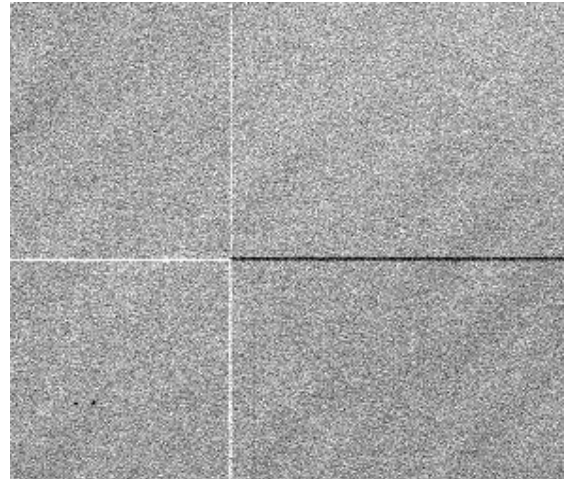


*Fig 1.1.16b Effect on a flat field, at X=1024 and Y=512*

The largest flux variation due to pixel size mismatch ever measured was 4%, leading to 2% of pixel size in both directions: 15.3x15.3  $\mu$ m, or in the worst-case 15.6x15  $\mu$ m. This makes a step in the overall CCD pixel geometry grid. Also pixel-to-pixel size variation may occur, but remains impossible to measure with a flat field due to an unavoidable correlation with pixel-to-pixel quantum efficiency variations. Nevertheless, local pixel-to-pixel and boundaries pixel size changes have never been so far noticeable in any astrometric calibrations (Wide field Imager, SUSI2 and UVES). Finally, these boundaries discontinuities can be calibrated forever, and can be used to correct the data.

## **2. The CCDs for HARPS**

## **2.1. CCD #1**

The first EEV44-82 CCD (SN 8131-18-1) has been nicknamed JASMIN and is meeting all the expectations performance-wise.

### **2.1.1. QE**

QE has been measured using ESO's CCD testbench. The device QE is well according the mean of all the devices measured.

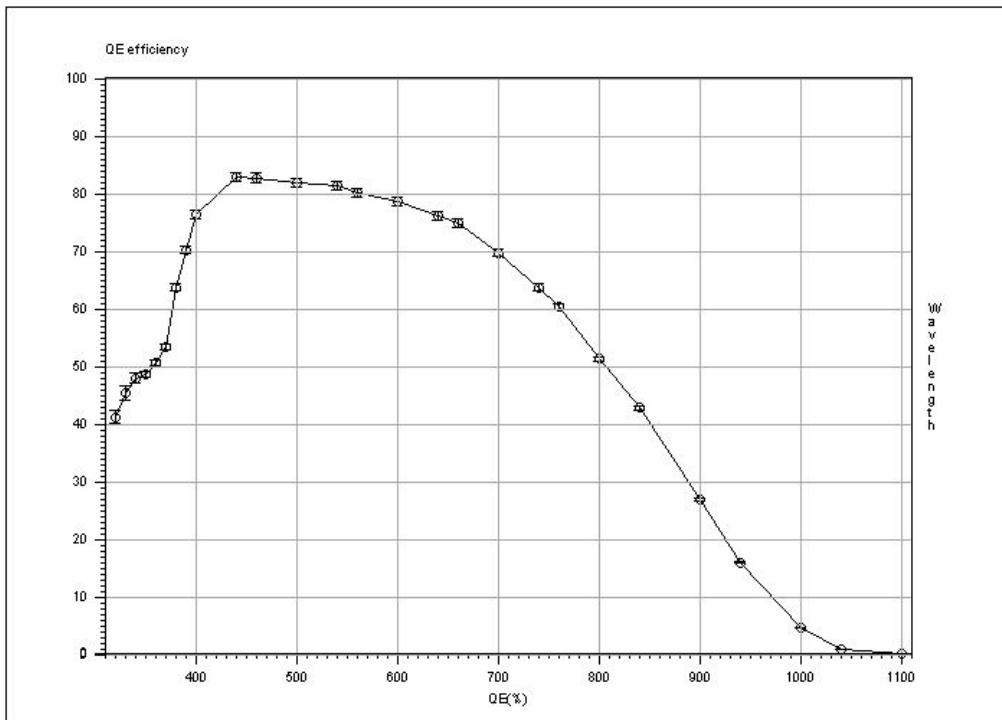


Figure 2.1.1 Jasmin's QE

### **2.1.2. Noise**

Noise has been measured by EEV and ESO. EEV figures are 2.1e- noise for both ports at 25Kpx/s ESO has means to read it out much faster, the testing speed was 350kpx and the noise was around 4.1e- on both ports.

### **2.1.3. Linearity**

Adjusting CCD voltages can lower noise; nevertheless care has to be taken so that linearity is not too much degraded; that's why this parameter should be checked. Hereafter, measurement of linearity has been carried out.

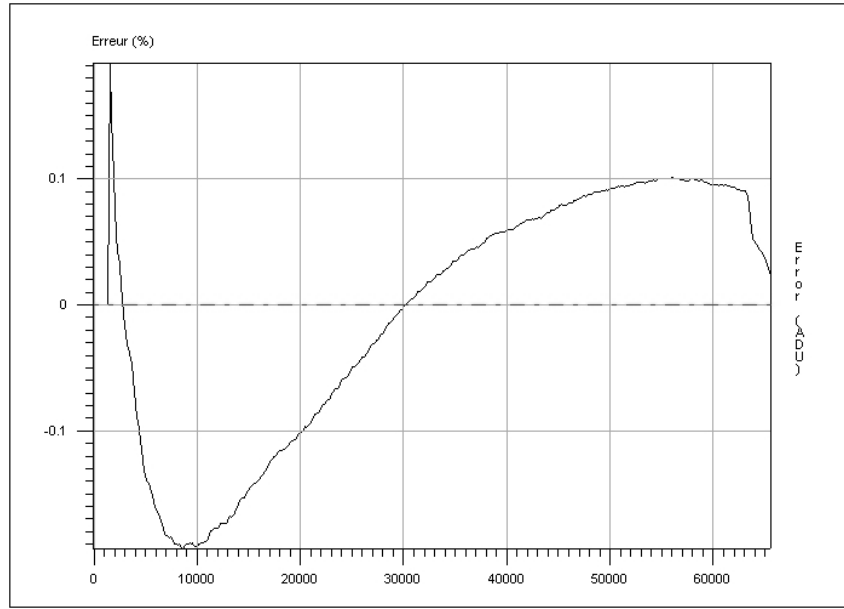


*Figure 2.1.3 Jasmin's non linearity*

It exhibited non linearity of less than +/-0.2% peak to peak for a range of 125000 e- (ie 65535 adus).

#### **2.1.4. Flatness**

The flatness of the device has been measured by EEV. The peak to valley is about 12 $\mu$ m.

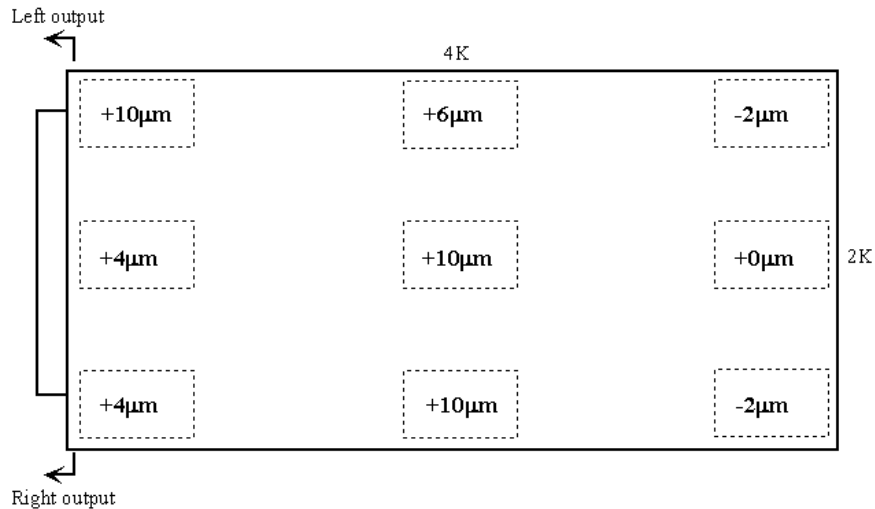


*Figure 2.1.4 Jasmin's flatness*

#### **2.1.5. CTE**

CTE has been measured at 166kpx/s and showed horizontal CTE of 0.999999 and vertical CTE of 0.99999942.

#### **2.1.6. Dark Current**

No tests have been carried out, but dark current less than 2e-/pix/hour is expected.

#### **2.1.7. Cosmetic defects**

This device exhibits very few defects and has :

- 3 Traps/hot columns starting at (unit in mm) : X=9.930, Y=44.955, X=25.005 Y=8.73, X=30.345, Y=28.65 and (origin located at the bottom left amplifier at pixel 1-1) White squares on figure 2.1.7 shows starting point of the traps.
- Bias frame is almost free of any defects (bright column at X=25.005 Y=8.73)
- Long dark frame : not available, but likely same defect as the bias frame.
- Some 10 to 100 pixels vertical and horizontal pixels in a row having a loss of 20% of QE (these flat field-out perfectly), shown as stars on figure 2.1.7.

FITS sample files can be provided upon request.

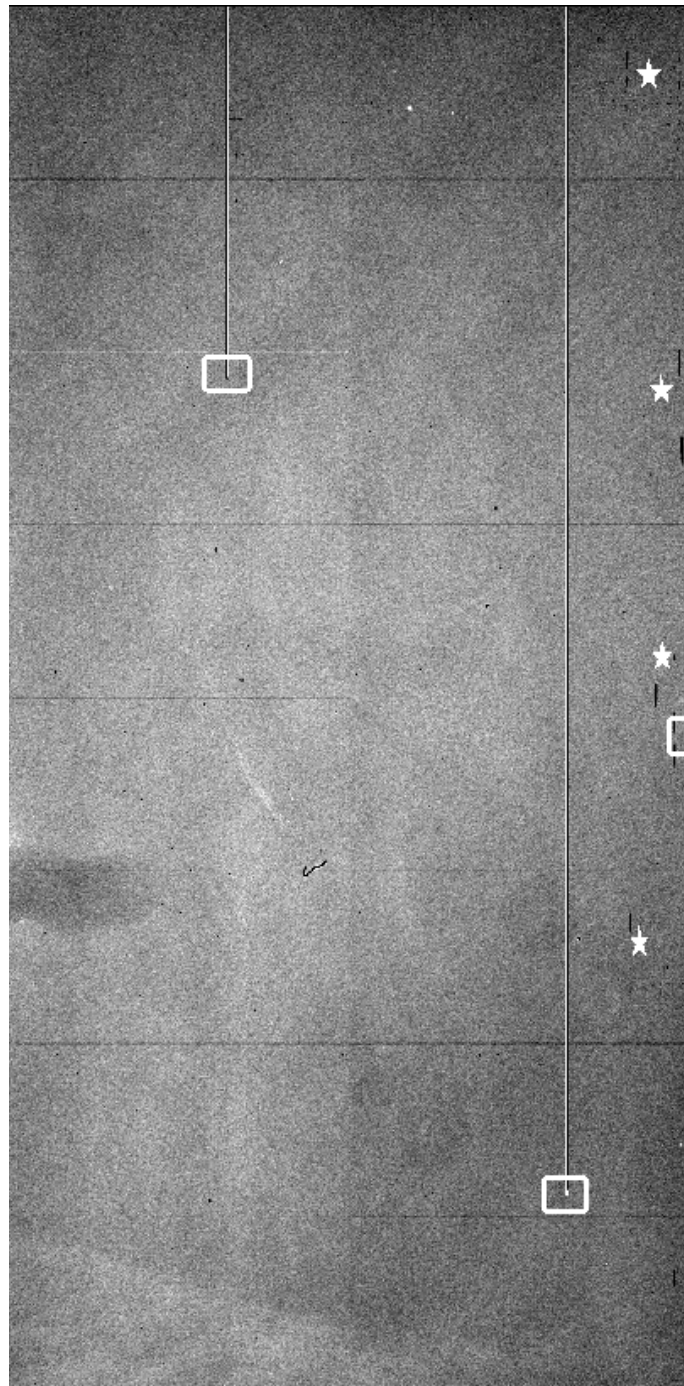


Figure 2.1.7 Jasmin's flat field, 2% saturation level, 650nm, 5nm bandwidth

## **2.2. CCD #2**

The second EEV44-82 CCD (SN 8131-13-1), from the same lot as the previous one, has been nicknamed LINDA and is also meeting all the expectations performance-wise as a science grade device.

### **2.2.1. QE**

QE has been measured using ESO's CCD testbench. The device QE is well according the mean of all the devices measured.

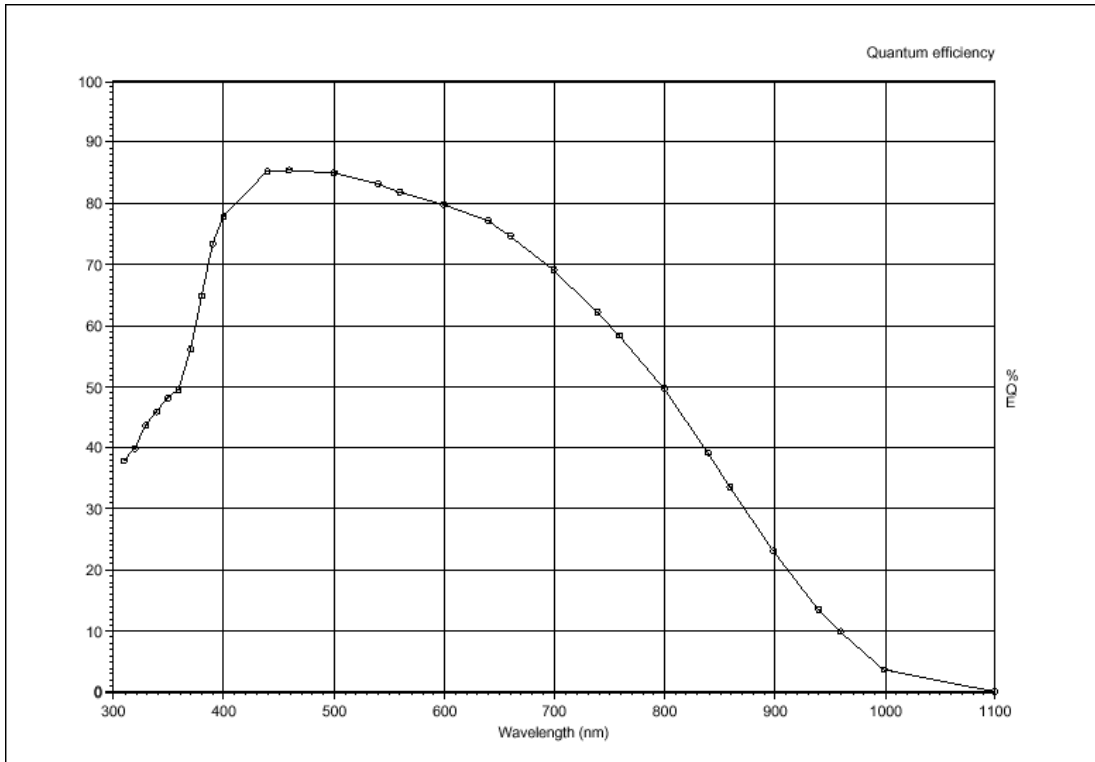


*Figure 2.2.1 Linda's QE*

### **2.2.2. CTE**

CTE has been measured at 166kpx/s and showed horizontal CTE of 0.9999987 and vertical CTE of 0.99999948.

### **2.2.3. Dark Current**

Tests have been carried out, and dark current measured was less than 2e-/pix/hour.

### **2.2.4. Linearity**

Adjusting CCD voltages can lower noise; nevertheless care has to be taken so that linearity is not too much degraded; that's why this parameter should be checked. Hereafter, measurement of linearity has been carried out.

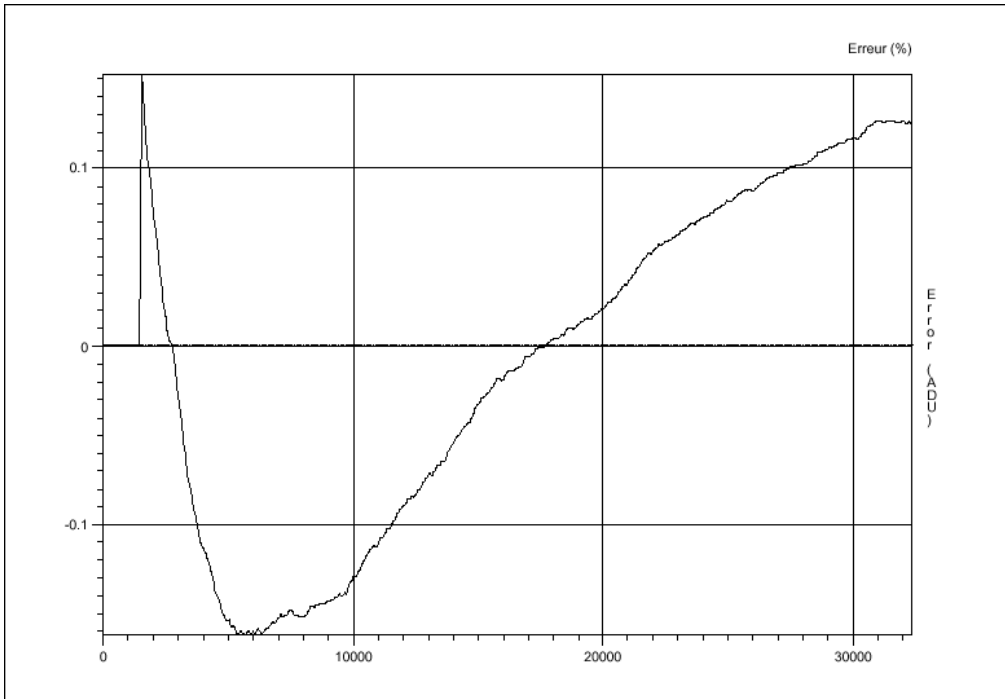


*Figure 2.2.4 Linda's non linearity*

It exhibited non linearity of less than  $\pm 0.2\%$  peak to peak for a range of 125000 e- (ie 65535 adus).

### **2.2.5. Flatness**

The flatness of the device has been measured by EEV. The peak to valley is about  $14 \mu\text{m}$ .

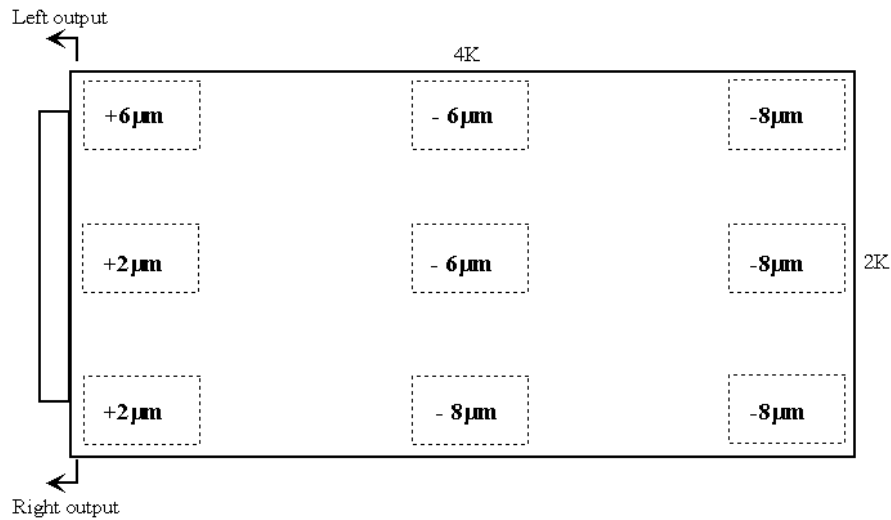


*Figure 2.2.5 Linda's flatness*

### **2.2.6. Noise**

Noise has been measured by EEV and ESO. EEV figures are  $2.1\text{e-}$  noise for both ports at 25Kpx/s  
 ESO has means to read it out much faster, the testing speed was 350kpx and the noise was around  $4.2\text{e-}$  on both ports.

### **2.2.7. Cosmetic defects**

This device exhibits very few defects and has :

- 2 Traps/hot columns starting at (unit in mm) : X=0855 Y=10.875 and X=13.95, Y=52.11 (origin located at the bottom left amplifier at pixel 1-1), white rounded rectangles in figure 2.2.7.
- Bias frame is free of any defects
- Long dark frame : a small tiny bright column at 25.48 and Y=24.31 (one hour exposure).
- Some 10 to 100 pixels vertical and horizontal pixels in a row having a loss of 20% of QE (these flat field-out perfectly) White stars in figure 2.2.7.

FITS sample files can be provided upon request.

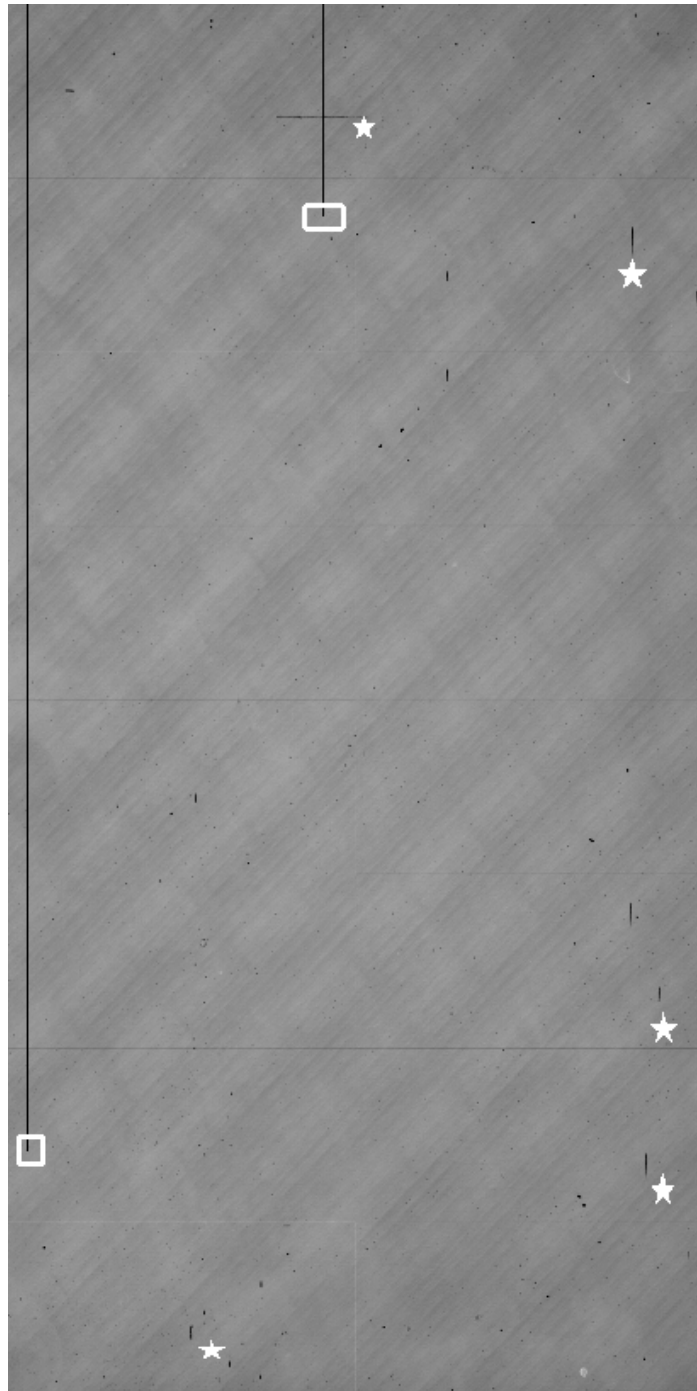


*Figure 2.2.7 Linda's cosmetics, 600nm flat field, 5nm bandwidth, 70% saturation level*

### 2.3. Readout modes and gains

Mode	Binning	Gain	Port/CCD	Speed Kpx/s	Noise (Expected) $e^-$	Readout time (sec)
#1	1x1	0.5	1	50	1.9 to 2.5	160
#2	1x1	0.5	2	50	1.9 to 2.5	80
#3	1x1	2.2	1	625	4 to 5	12.8
#4	1x1	2.2	2	625	4 to 5	6.4

### 3. The detector head

The detector head used will be a standard ESO CCD detector head and will be installed inside the vacuum chamber of the spectrograph. This complicates the way the cables have to reach the detector head, and more likely an additional vacuum cable feed through will have to be designed. A critical point concerns the video cables coming out from the CCD outputs, if those are too long, noise performance can be degraded, especially at high speeds. In that goal, shortest distance must be kept between the head and the preamp box (see 5.2.1).

Finally, the detector head is a standard ESO one, except the last top flange, which contains the field lenses instead of the flat entrance window.

#### 3.1. CCD holder re-design

The CCD carrier table has been redesigned in order to withstand the high geometric stability requirements. A monolithic aluminium part will be fabricated in that scope. It will consist of a merging of the aluminium part (VLT-DWG-ESO-13600-260000-0004) and the invar plate (VLT-DWG-ESO-13600-260000-0004) to a single aluminium part including space to install the heaters and temperature sensors. Hereafter the drawing of this new part:

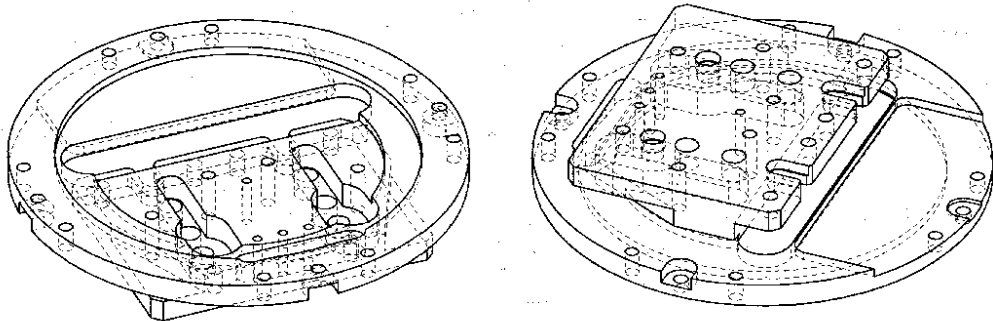


*Figure 3.1 New CCD holder prototype with temperature sensors.*

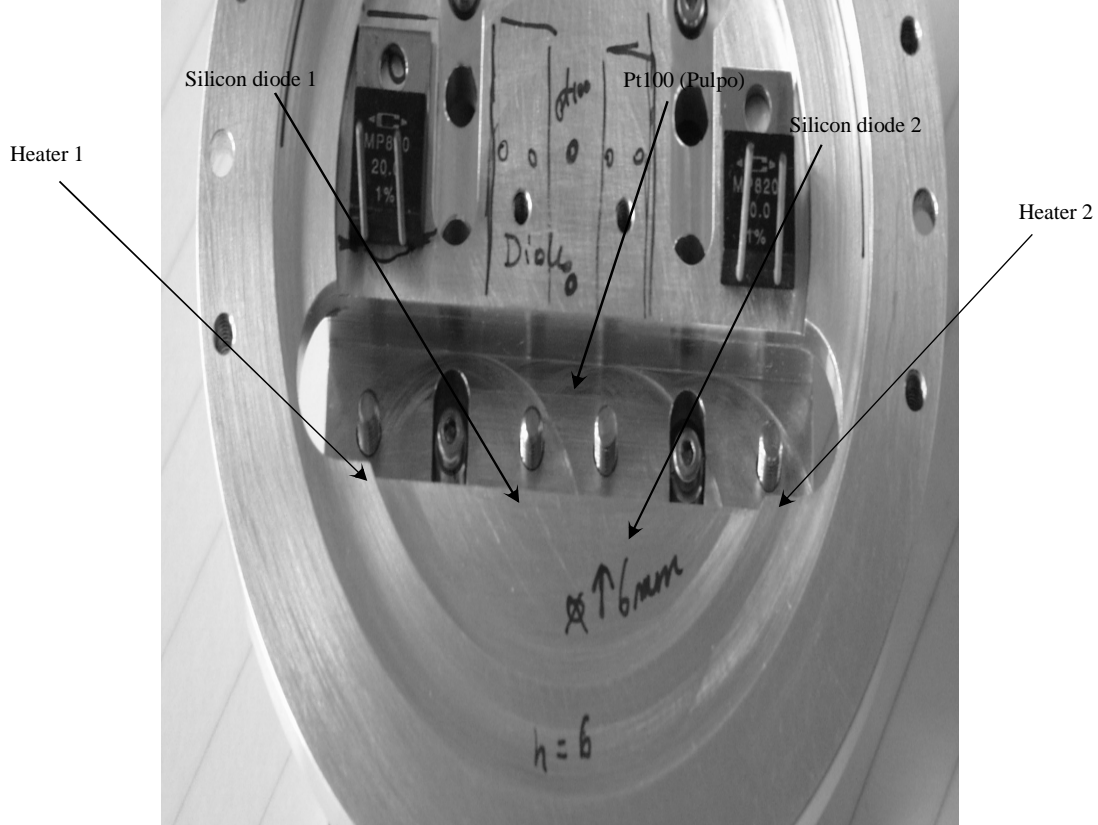


*Figure 3.1a Prototype of the New CCD holder, upside down.*

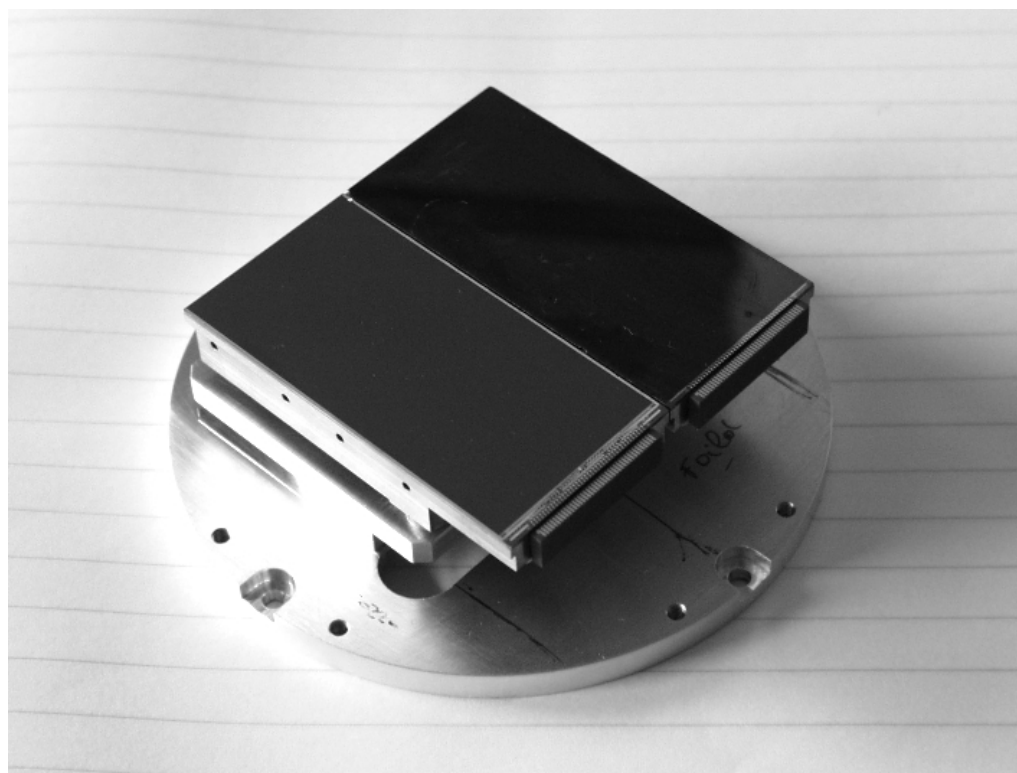


*Figure 3.1b Prototype of the New CCD holder, top view with two mechanical sample CCDs.*



*Figure 3.1c Prototype of the New CCD holder, side view with two mechanical sample CCDs.*

This one fulfils the requirements concerning the CCD gap, and also accommodates the two diodes for temperature sensing thru the Lakeshort controller, a pt100 for PULPO compatibility during maintenance operation and two heaters required for temperature stabilisation that can be operated either by Pulpo or the LakeShort controller (not at the same time).

### **3.2. The field lens and CCD's optomechanical requirements for HARPS**

According to the optical design, instead of having a flat entrance window, a field lens located at approximately 10 mm from the CCD surface will be installed instead. This lens behaves both as the last optical element of the optical chain and the vacuum seal from the outside world.

### **3.3. Contamination issues and recommendations**

In order to avoid the contamination of the CCD device while being operating at -120C, precautionary measures should be taken considering the backside surface of the field lens holder (called also Field lens unit):

The use of black anodization on the backside surface holder is forbidden, or in different terms, the side of the lens holder, which looks to the CCD, being inside the vacuum. Some machining oil or water can be trapped in the lens holder surface interstices. In the vacuum, these molecules evaporate, migrate and stick to the very cold CCD surface. A layer of optical active contaminant grows over the CCD surface gradually. After some weeks, the CCD quantum efficiency degrades, strongly in the U bands and images cannot be flat fielded properly.

To avoid this major degradation, the lens holder surface should be as smooth as possible and polished. Moreover, the whole lens holder, before mounting lenses, should be cleaned by baking it in the vacuum oven at 200C, to remove all the remainder grease from machining.

The grease used to seal the o'ring to the lens and to the holder must be a special vacuum grease (vapour pressure of  $10^{-12}$ )

### **3.4. CCD mosaicing considerations and positioning tolerances**

Two CCDs will be installed close together to fill the focal plane. The following drawing explains how the CCD will be laid out :

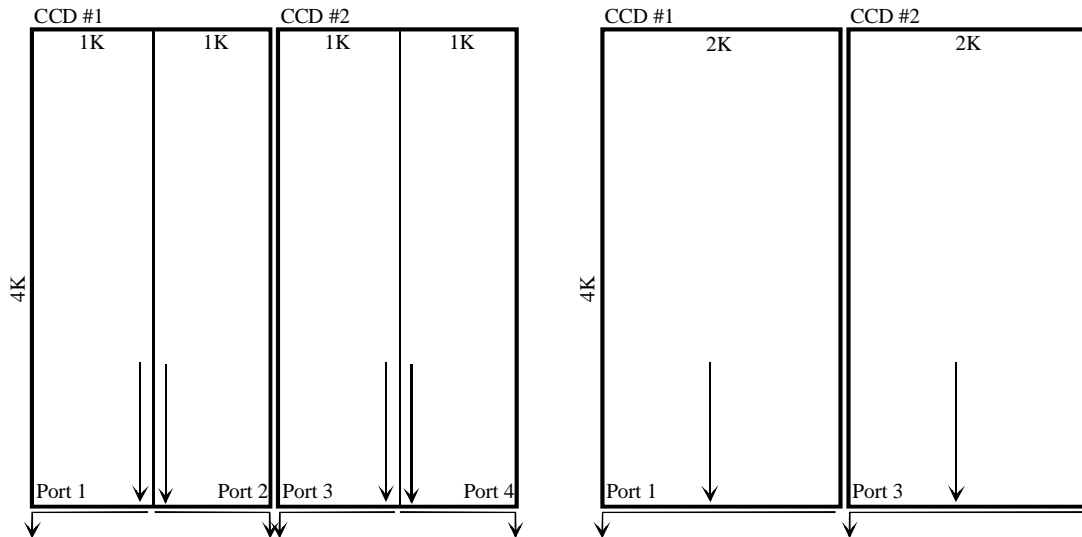


*Figure 3.4, readout modes geometry*

According to our experience with the mosaic of 8 EEV44 CCDs (Wide field Imager), the mean CCD to CCD tilt achieved was 8 arcmin (10 pixels to the long side) and X and Y shifting kept within 75  $\mu\text{m}$ . All these misalignments are due to intrinsic mechanical tolerances including CCD package and drills into the holder plate.

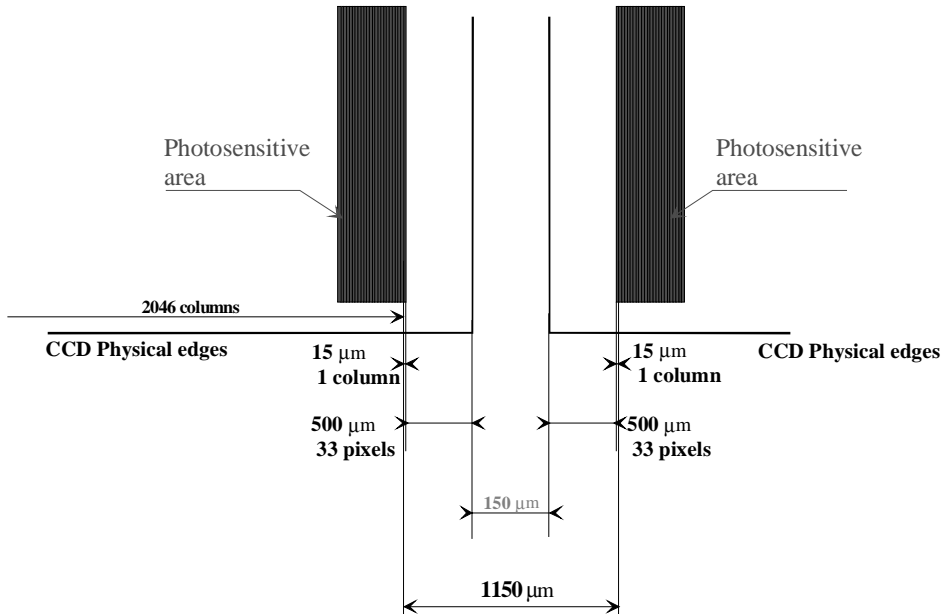


*Figure 3.4a Close up of the gap between two CCDs*

The physical distance between two devices has lowered to  $150\mu\text{m}$ , added to the fact that the photosensitive area is located at  $500\mu\text{m}$  from the edges; it leads to a CCD to CCD total lost space of  $1170\mu\text{m}$  (78 pixels). The inter-CCD gap cannot be reduced to under these figures, because when mounting the devices on the carrier plate, they could be damaged seriously if contact occurs between them.

The flatness tolerances are based upon a maximum allowable defocus blur of  $10\mu\text{m}$  with a target of  $5\mu\text{m}$ , due to the fact that the optics will deliver 80% of the energy within a circle of  $15$  to  $20\mu\text{m}$ . The distance of two planes, parallel to the reference flange, between which the sensitive surface of the chip is contained can be kept less than  $30\mu\text{m}$ . This applies to optical field size only.

### **3.5. Output connectors and orientation**

There is different kind of vacuum connectors going out from the head: a temperature connector ( $\varnothing 28.6\text{ mm}$ ), a clock connector ( $\varnothing 35\text{ mm}$ ), a bias connector ( $\varnothing 28.6\text{mm}$ ) and a video connector ( $\varnothing 28.6\text{mm}$ ). The Temperature, bias and clock connectors **have fixed positions** according to the CCD. The video connector could be installed in one of the holes mentioned in figure 3.5 so as to minimize the length to the preamp box, which is supposed to be outside the vacuum chamber of the spectrograph.

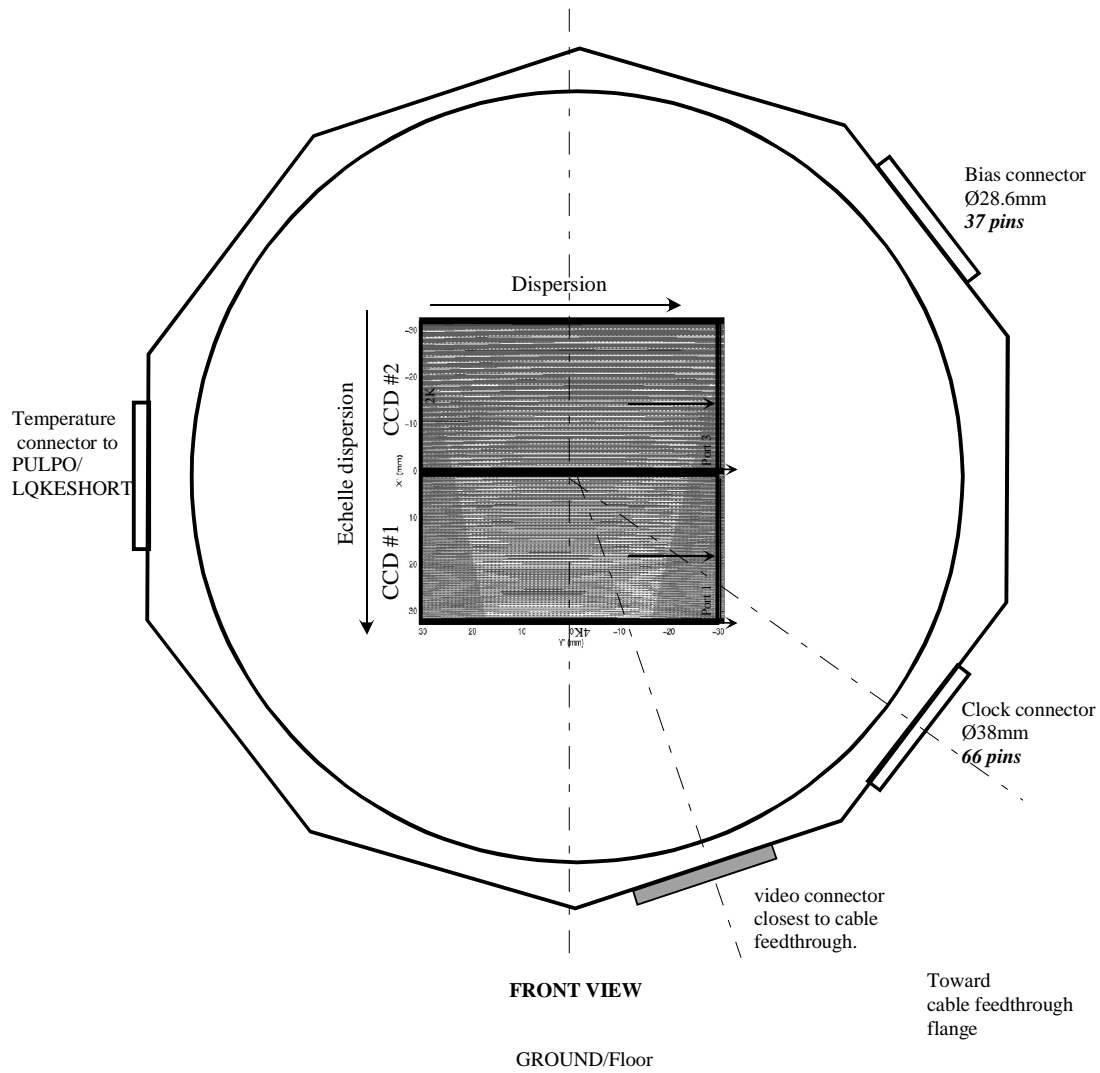


*Figure 3.5 - CCD head orientation, connectors, spectra dispersion relative to ground/floor*

More information about interfaces will be found in the HARPS Interface Document Control about connectors and their way to FIERA.

#### 4. The cryostat

The cryostat aims to cool down the CCD at  $-120^{\circ}\text{C}$ , is a continuous flow type (CFC). ESO's integration team will make this cryostat. The document concerning the CFC controller can be found in the ESO archive.

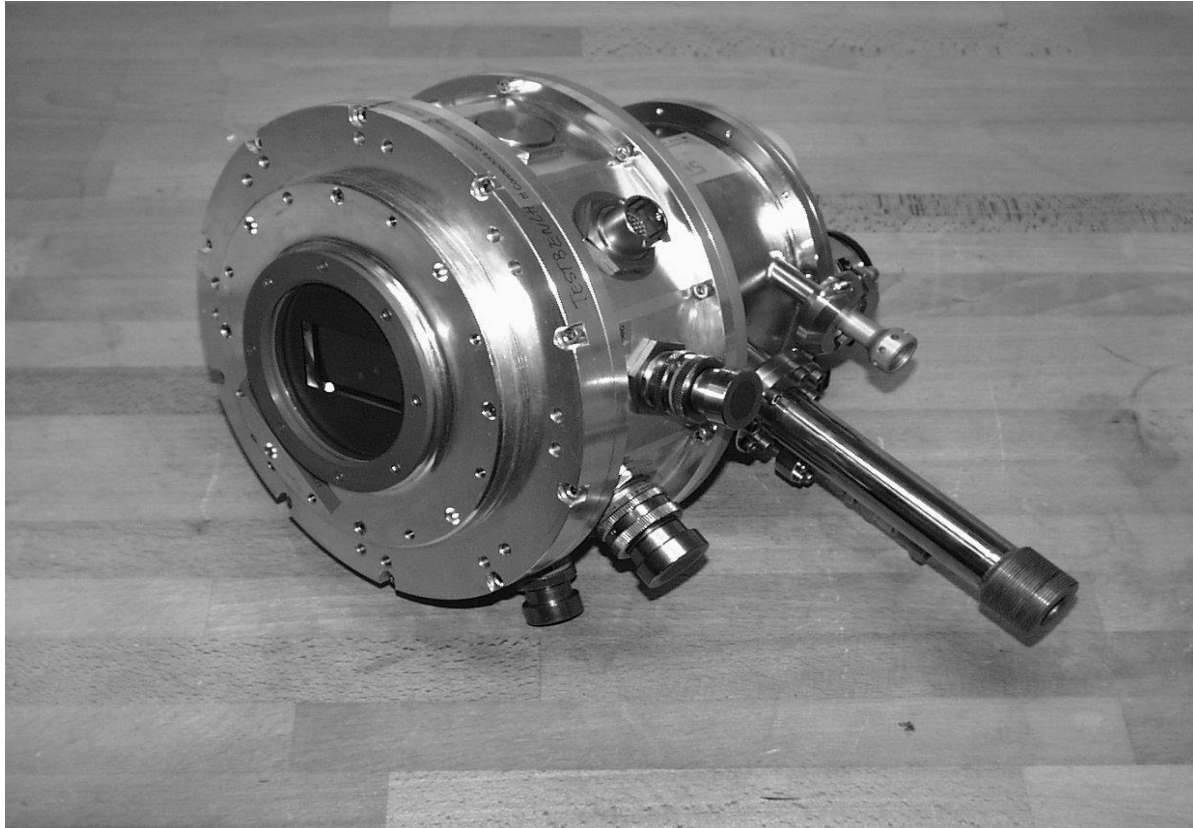


Figure 4

*CFC cryostat to be used for HARPS, the head (left part) and the continuous flow cryostat (right part) will be split and re-tied by a special vacuum link.*

#### 5. FIERA System

##### 5.1. General overview

The Purpose of the next section is to give an overview about Fiera System and hardware, a more complete document can be found at ESO archive as VLT-MAN-ESO 13640-1845 and VLT-MAN-ESO 13640-1844.

The fundamental goal for FIERA is to make a controller that can optimally operate any CCD chip or mosaic that ESO acquires for the next 10 years. The limitation of the entire detector system is due solely to the CCD and the imagination of the user. The electronics (hardware and software) of FIERA should be transparent to the user. We list here some of the specifications of the FIERA design:

- 40 MHz fundamental clock

- Up to 32 readout ports
- Up to 40 Mpixel/sec total
- Up to 21 bits/pixel
- Up to 5 Mpixel/sec/port
- Initially 1 MHz pixel rate limitation at 16 bits per pixel (set by A/D limitation)
- Readout noise must be dominated by the CCD device for both slow and fast readout; the electronic noise must be negligible
- Fully programmable high current clock drivers (25.5V swing, 0.1V resolution at 40 MHz, 2 amps instantaneous per driver)
- Nearly unlimited number of control bits (at 40 MHz)
- Analog biases fully programmable with hardware limits on potentially damaging biases
- 4 gain settings
- 64k offset levels
- 4 low pass filter settings (can optimize clamp & sample at 4 speeds)
- Gbit/sec fiber optic data link from detector head to embedded computer
- Embedded telemetry and test signals
- No software in the detector head / minimalistic design
- Fully modular and expandable.

The FIERA controller consists of three modules:

1. A set of detector head electronics that will be mounted as close to the CCD as possible, preferably on the CCD cryostat itself. If there is too much distance between these electronics and the CCD, we will use pre-amplifiers to boost the video signal for low noise performance.
2. A DC power supply module that generates a set of clean voltages for the detector head electronics. This power supply should be within 3 meters of the detector head electronics.
3. The detector computer with a custom made computer interface board. The interface board contains a Gbit/sec duplex fiber link and two C40 DSP chips for system control and interface to external computers / processors. The distance of the fiber optic data link between the detector computer and detector head electronics can be up to 500 meters with standard parts, up to 20 km with pin compatible upgrade to more expensive transmitter / receivers.

In the system we have to custom designed printed circuit boards; the computer interface board and five boards in the detector head :

- i   Communications board (fiber link and bus interface)
- ii. Clock drivers
- iii. Analog biases
- iv. Video processing (amplification, gain, offset, correlated double sampling, digitization)
- v. Custom backplane

A good feature of the system is that there is no software or processors in the detector head. The detector head runs via an "extended bus" structure provided by the Gbit/sec data link. All system "smarts" reside in the C40 sequencer chip and the SPARC computer that is used as the dedicated computer for the system.

## **5.2. FIERA for HARPS**

The figure shows the general physical architecture of the whole system. The following section is a short summary about the role of each part.

**Part 1 :** This part concerns the optical head and the cryostat described in the previous section

**Part 2 :** This part is a small box, called preamp box, having the goal to amplify to CCD output signals, here 2 channels. This preamp box is located at 10 to 50 cm from the CCD head.

**Part 3 :** The FIERA box provides all the clocks and biases voltages to read out the CCD, and to digitize the analog signals coming from the preamp box. This box is also relatively close to the CCD head, less than two meters. This box is water-cooled (see section 5.3). The Harps detector head box will contain:

Item	Amount	Information
Video Board	1	4 ADC channels
Bias Board (32 biases)	1	22 biases
Clock Board	2	26 clocks
Communication board	1	Standard

**Part 4 :** This is the DC power box to supply all the DC voltages to the FIERA box (part4). This box is nearby to the FIERA box, less than two meters. This box is water-cooled (see section 5.3).

**Part 5 :** The PULPO controller aims to regulate and monitor the CCD temperature, the cryostat temperature, the cryostat vacuum level. This unit is tied to every part of the system. In HARPS instrument, PULPO will only read the temperature (Accuracy 0.1C) and monitor the cryostat pressure. A LAKESHORT controller provided by Geneva Observatory will achieve the final CCD temperature control. This controller allows an accuracy of +-0.01C. It will be up to Geneva Observatory to take care of the software integration of this control thru the Instrument Control Software. ODT will implement underneath the CCD, PT100 and heating resistor to allow to able the LAKESHORT controller to regulate properly the CCD temperature. The shutter will be more likely a SESO shutter as used for UVES and the VLT tests cameras.

**Part 6 :** Coming out from the FIERA box, a fiber link going to this part #6: FIERA SPARC System Local Control Unit. This is the FIERA brain, sending order to the FIERA box, receiving data and sending them out thru the network. This box could be located far away from the detector head, thanks to the fiber link.

**Part 7 :** The Continuous Flow Cryostat (CFC) needs to have the liquid LN2 going in to be accurately controlled by this device. It is located close to the detector head.

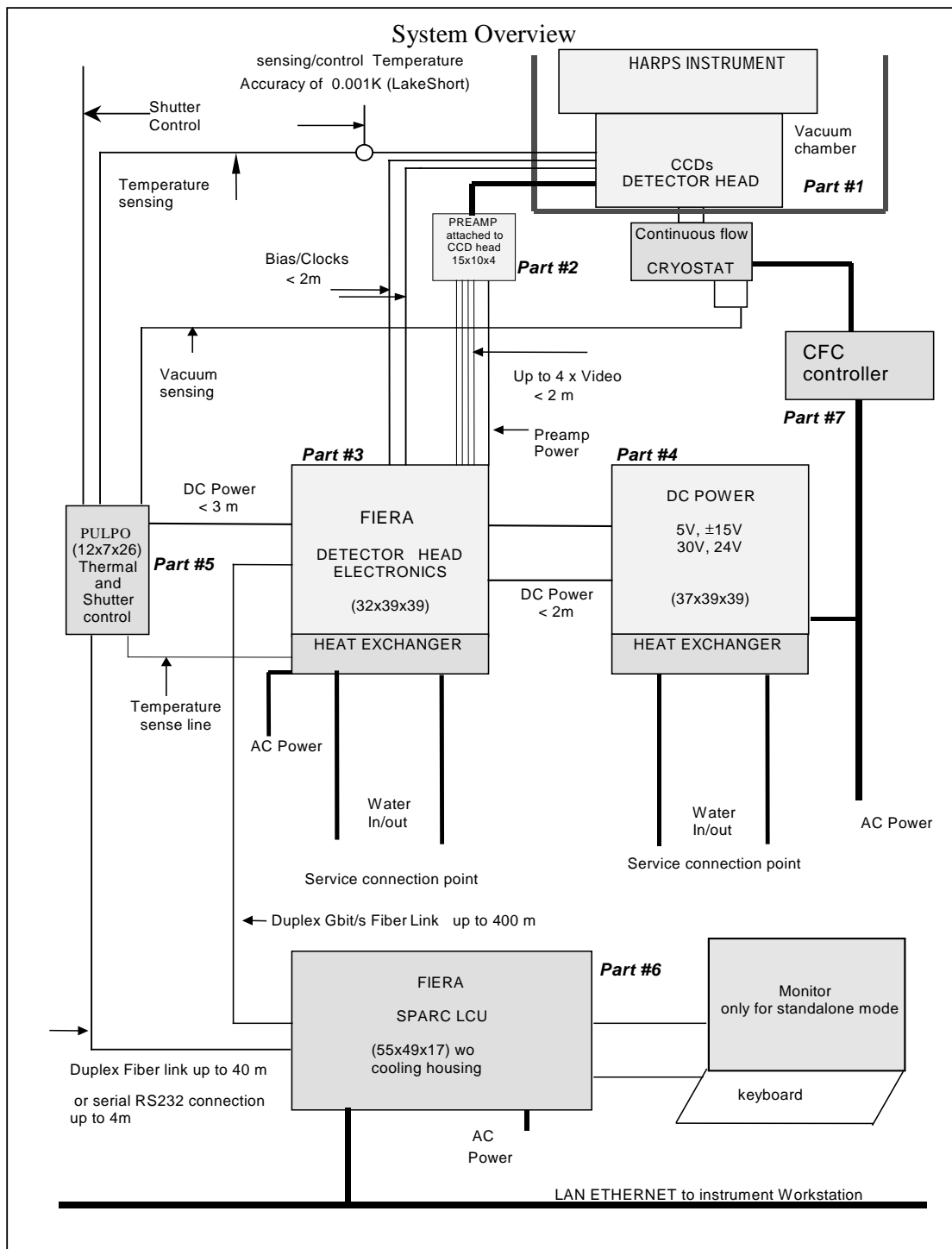


Figure 5.2 System general overview

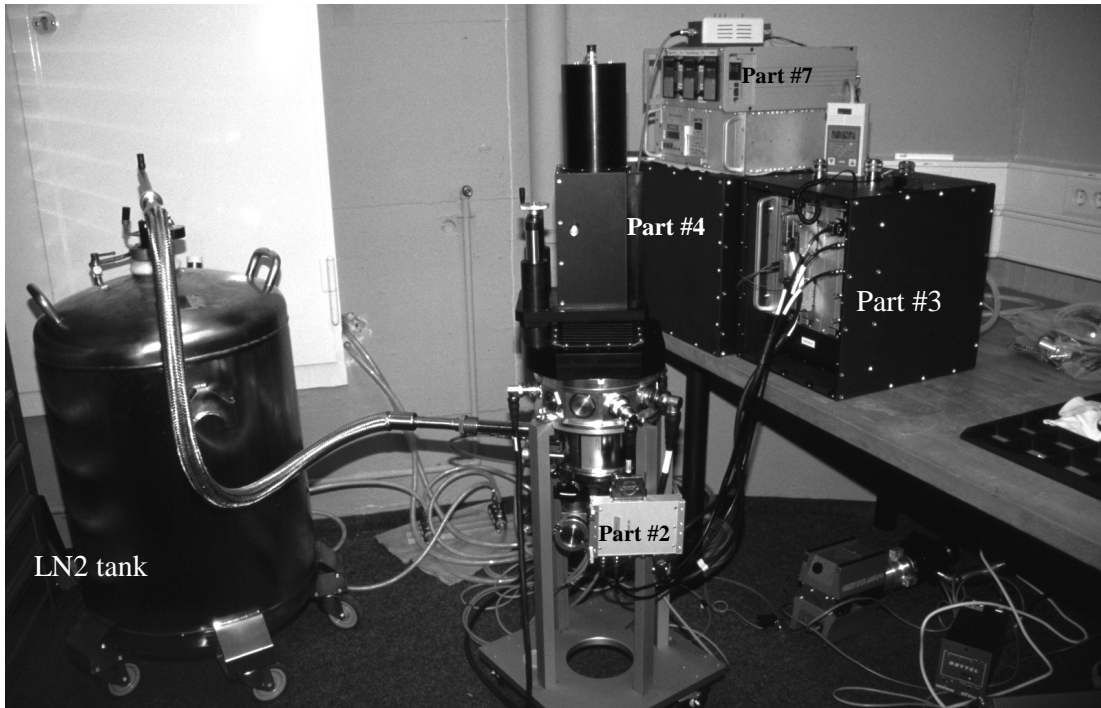


Figure 5.2a CCD detector system using a CFC cryostat

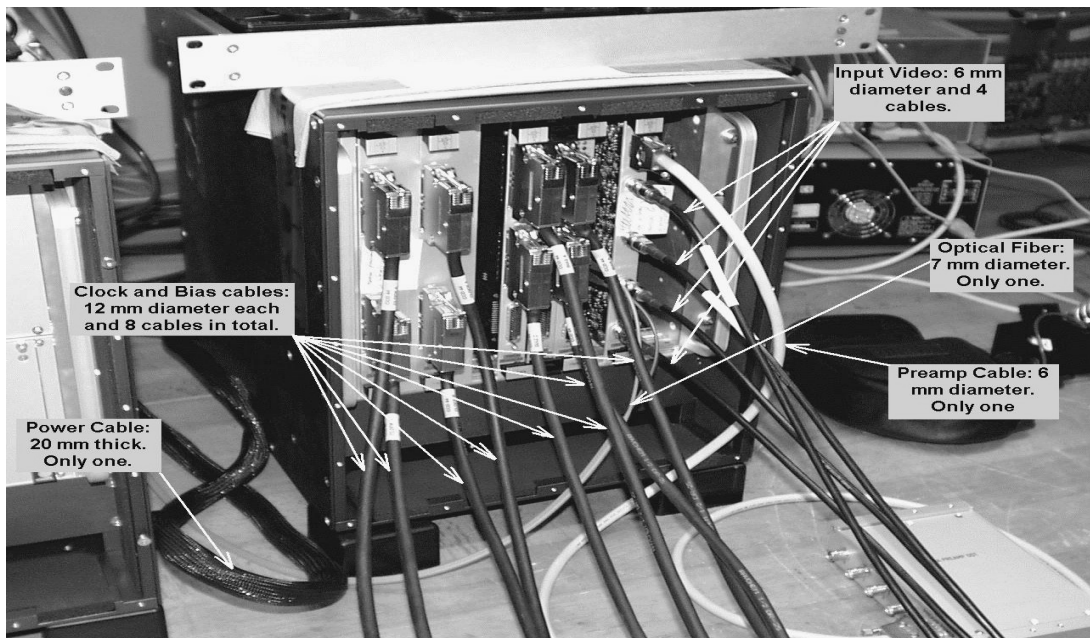
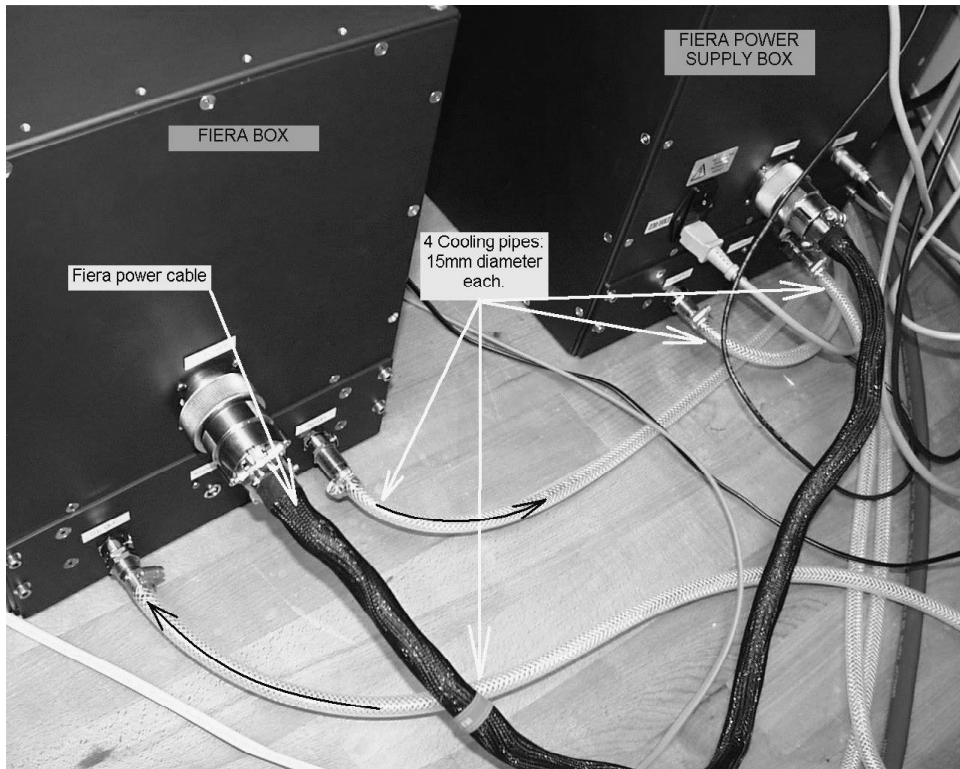


Figure 5.2b FIERA Box, Part #3 these picture shows four video cables.

### **5.3. FIERA Housing and cooling**

These technical notes describe the basic design and performance of the FIERA Housing and Cooling system. The optical detector team has developed an active cooled housing for the CCD systems to meet the temperature specifications for the VLT. Fiera Box, Fiera Power supply and the SUN-Sparc box (if required because being close to the instrument/telescope) must be cooled to avoid any additional turbulence or unwanted source of heat.

The FIERA active water-cooling system acts like a typical closed loop liquid cooling system. In a typical closed loop air cooling system cool water is supplied to the heat exchanger and (filtered) air is circulated between an electronic enclosure and a heat exchanger, which then transfers the heat to water flowing through the tubes. Our heat exchanger is placed inside the enclosure with cooled exit air blown directly through the FIERA boards and power supplies. This system permits closed loop air-cooling and prevents entry of contaminated intrusion air.



*Figure 5.3 Cooling and main power supply of part#3 and #4*

Heat exchangers require some temperature difference between liquid and air entering the heat exchanger. In the VLT environment the incoming water temperature of the heat exchanger is regulated to be always 8 degC below the ambient temperature. In order to dissipate all the thermal energy produced the thermal performance of the FIERA heat exchanger was specified as following. To rate the thermal performance (TP) of our heat exchanger the following assumptions and equations was applied:

$$TP \text{ [Watts/}^{\circ}\text{C}] = \frac{Q}{T_{\text{air in}} - T_{\text{water in}}} = \frac{\text{Thermal energy produced by the boards or power supplies}}{\text{Air temperature into HX} - \text{Watertemperature into HX}}$$

Figure 1 shows the FIERA heat exchanger mounted on the Rack unit. The heatexchanger is equipped with 4 slim-line low noise fans to blow air through the complete area of the electronic boards. The fans

are wired in parallel and operated with 24V DC voltages. The operating temperature range is from -10 degC to +70 degC. Additionally a temperature sensor (PT 100) is mounted on the rack on a cooling profile. This sensor monitors the air temperature inside the box and will give the reference value for the flow control unit.

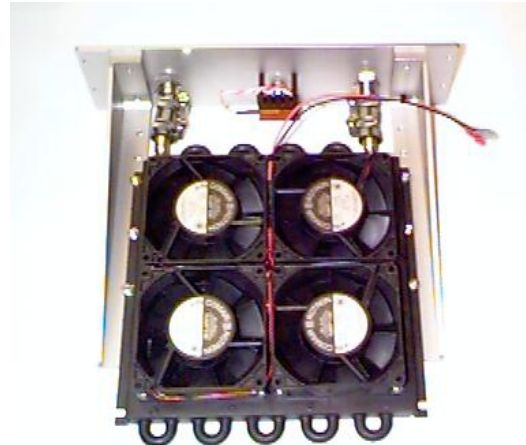


*Figure 5.3a Cooling of part#3 and #4*

Will dissipate 200 Watts as a maximum value with a fully equipped FIERA detector head (11 slots) or power supply box. With an initial temperature difference of 8 degC the heat exchanger must have a minimum thermal performance of  $200 \text{ watts} / 8 \text{ degC} = 25 \text{ Watts/degC}$ . The result from the custom made heat exchanger is a little bit better and has TP of 27 Watts/degC. Thus  $200 \text{ Watts} / 27 \text{ Watts per degC} = 7.4 \text{ degC}$ . This means that the heat exchanger will dissipate 200 Watts and require 7.4 degrees C difference between the incoming water and incoming air. If the incoming water temperature is constant at 10 degC, the incoming air will stabilize at 17.4 degC.

#### 5.4. Harps shutter

The Harps shutter is a SESO shutter model that has been previously used at UVES. This is a blade iris type shutter driven by a controller. This shutter is well suited for still operations (ie the shutter does not move). PULPO can control properly the shutter, including opening delay feedback and so on.

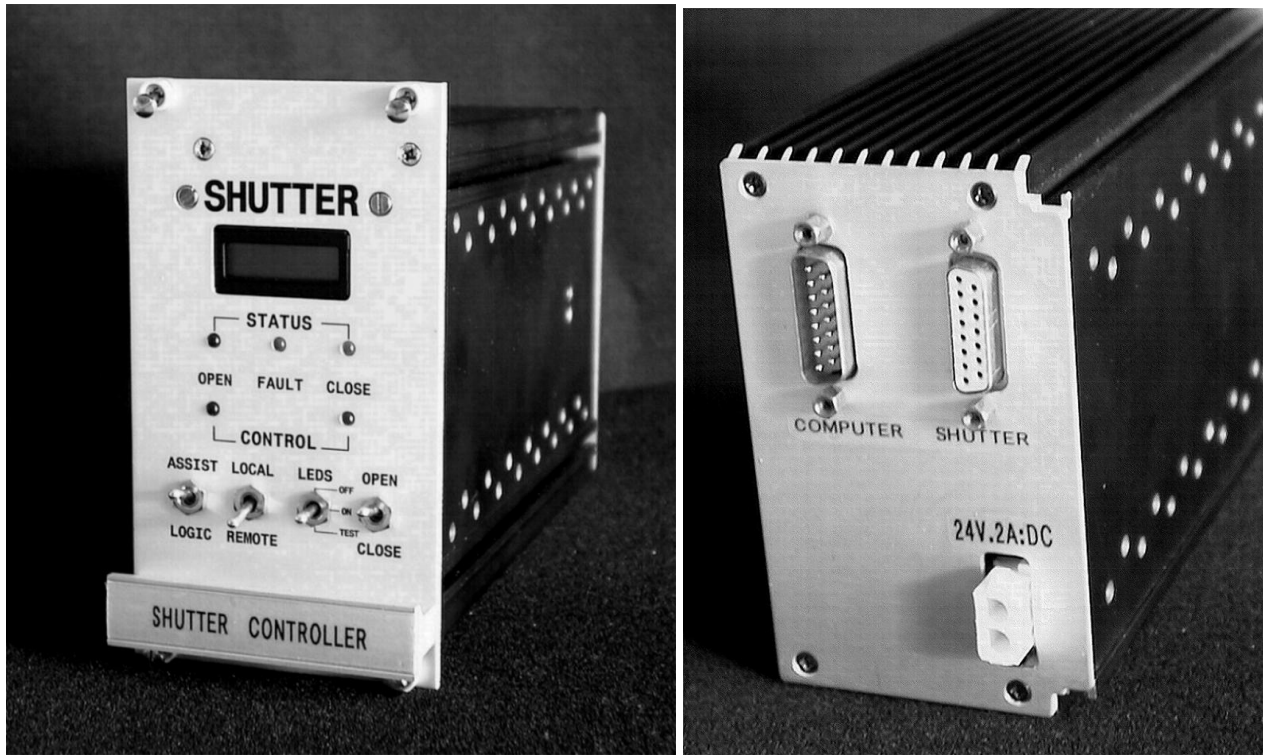


*Figure 5.4 SESO Shutter controller, front and back panels*

### **5.5. FIERA racks and boxes in the spectrograph's room**

All the FIERA components placement is shown in the 3M6-TRE-HAR-33100-0003\_V1,1 document page 162, figure 49.

#### **5.5.1. Detector head boxes, PULPO**

The two blue detector head boxes (part#3 and #4) and Pulpo will be located nearby to the HARPS vessel, concerns must be taken into account concerning cable length to CCD head.

#### **5.5.2. FIERA LCU (Part #6)**

FIERA Local Control Unit (LCU) is SPARC that includes a PCI bus. This LCU includes a PCI board that owns all the features/components to control the detector head box : DSP, fibre input, data capture interface, PULPO fibre input, TIM module. The whole racks measures: 44cm depth, 43cm length, and 17cm height.



*Figure 5.5.2 FIERA LCU*

### **5.5.3. Continuous Flow Cryostat (CFC) controller (Part #7)**

In order to regulate the LN2 cold plate, head vacuum, zeolithe regeneration, Ln2 tap and Ln2 level in the tank, a CFC controller has been designed by the ESO technical division. This CFC controller must be installed into the HARPS rack, nearby the CFC. More information in VLT-MAN-ESO 171300-2345, VLT-MAN-ESO 13200-1969 and VLT-MAN-ESO 13200-1970 can be found.



*Figure 5.5.3 CFC controller*

## **6. References**

Additional information can be found through internet at <http://www.eso.org/projects/odt> concerning FIERA and CCDs. Also ESO archive could be referred for any VLT-MAN-ESO documents.

